Extensional exhumation of cratons: insights from the Early Cretaceous Rio Negro-Juruena belt (Amazonian Craton, Colombia)

Ana Fonseca[1], Simon Nachtergaele[1], Amed Bonilla[2], Stijn Dewaele[1], Johan De Grave[1]

[1]Laboratory for Mineralogy and Petrology, Department of Geology, Ghent University, Ghent, 9000, Belgium
[2]Servicio Geológico Colombiano, Dirección de Recursos Minerales, Bogotá, Colombia

Correspondence to: Ana Fonseca (anacarolina.LiberalFonseca@ugent.be)

Abstract. This study presents results from apatite fission track (AFT) thermochronology to investigate the thermal history and exhumation dynamics of the Rio Negro-Juruena basement, situated within the western Guiana Shield of the Amazonian Craton. AFT dating and associated thermal history modelling in South America has largely been restricted to the plate's margins (e.g. Andean active margin, Brazilian passive margin and others). Our paper reports on low-temperature thermochronological data from the internal part of the western Guiana Shield for the first time. This area is part of a vast cratonic lithosphere that is generally thought to be stable and little influenced by Mesozoic and Cenozoic tectonics. Our data however show AFT central ages ranging from 79.1 ± 3.2 Ma to 177.1 ± 14.8 Ma with mean confined track lengths of ca. 12 µm. Contrary to what might be expected of stable cratonic shields, inverse thermal history modeling indicates a rapid basement cooling event in the early Cretaceous. This cooling is interpreted as a significant exhumation event of the basement that was likely driven by the coeval extensional tectonics associated with back-arc rifts in the Llanos and Putumayo-Oriente-Maranon basins. The extensional tectonics facilitated both basement uplift and subsidence of the adjoining basins, increasing erosional dynamics and consequent exhumation of the basement rocks. The tectonic setting shifted in the late Cretaceous from extensional to contractional, resulting in reduced subsidence of the basins and consequential diminishing cooling rates of the Guiana Shield basement. Throughout the Cenozoic, only gradual, slow subsidence occurred in the study area due to regional flexure linked to the Andean orogeny. Comparative analysis with low-temperature thermochronology data from other West Gondwana cratonic segments highlights that exhumation episodes are highly controlled by tectonic inheritance, lithospheric strength, and proximity to rift zones. This study underscores the complex interplay between tectonic events and the response of cratonic lithosphere over geological time scales and highlights extensional settings as an important geological context for craton exhumation.

1 Introduction

Cratons, originating from the Greek term 'kratos' denoting 'strength', are the vestiges of the Earth's initial lithosphere. While the term 'craton' is commonly applied to denote steady segments of Archean (>2.5 Ga) crust, its definition remains unbound by age connotations, since some of them might have only achieved their ultimate consolidation and stability in the Proterozoic (Bleeker, 2003). Traditionally, they are described as regions that have achieved and maintained prolonged periods of tectonic

30 and geomorphic stability, existing as relatively inert fragments of crust (e.g., Salazar-Mora et al., 2018, Manatschal et al., 2015; Artemieva, 2006; Kusznir and Park, 1984; ~~Artemieva, 2006; Manatschal et al., 2015; Salazar-Mora et al., 2018~~). The stability of cratons is thought to be partly influenced by their thicker lithosphere, often exhibiting a high effective elastic thickness that can exceed 100 km (Artemieva, 2006). Additionally, they are characterized by a relatively cold but compositionally buoyant upper mantle keel.

35 In the last few decades of the previous century, the paradigm of craton~~s'~~ stability started to be questioned, largely driven by the discovery of numerous unconformities in sedimentary sequences within intracratonic basin (Sloss, 1992, 1963). More ~~R~~recently, there has been an exponential increase in evidence that challenge~~s~~ ~~there has been increasing evidence challenging~~ the concept of enduring craton stability and suggesting periodic disturbance within cratonic settings (e.g., ~~Foley, 2008;~~ Hu et al., 2018; Liu et al., 2018; Snyder et al., 2017; Kusky et al., 2014; ~~Liu et al., 2018; Snyder et al., 2017~~Foley, 2008). Notably,

40 this evidence includes periods of rifting and the formation of intracratonic aulacogens, occurrences of Mesozoic and Cenozoic magmatism, reports of intracratonic earthquakes, and even elevation changes on the craton's surface (e.g., Rooney, 2020; Gordon et al., 2017; Ye et al., 2017; ~~Chimpliganond et al., 2010;~~ Ault et al., 2013; Chimpliganond et al., 2010~~Gordon et al., 2017; Ye et al., 2017; Rooney, 2020~~). In this context, Bedle et al. (2021) present two plausible explanations for craton deformation and instability: either the craton's initial formation lacked the necessary thickness, buoyancy, or strength to

45 maintain stability across dynamic conditions, or subsequent geological processes have altered its stability. Noteworthy among these destabilizing processes or conditions, as emphasized by Bedle et al. (2021), are shearing, proximity to buffer zones (e.g., orogens ~~or mobile belts~~), interaction with mantle plumes, and rifting. A significant aid in unravelling the chronological sequence of these events comes from low-temperature thermochronology, which effectively constrains the episodes of cooling and heating within the Earth's upper crust (see Kohn and Gleadow, 2019 for a review). These episodes of crustal cooling and

50 heating are closely linked to geological phenomena such as kilometer-scale erosion, sedimentary burial, faulting, and magma emplacement. As a result, low-temperature thermochronology play a pivotal role in providing insights into deciphering the intricate history of potential geodynamic processes influencing the (in)stability of cratons.

The Amazonian Craton is a vast craton exposed in the Amazonian rainforest in South America and was once part of the West Africa-Amazonian Craton (Santos et al., 2006; Tassinari and Macambira, 1999) ~~(Fig. 1)~~. It can be subdivided into the Guiana

55 Shield to the north of the Amazon River Basin and the Guaporé Shield to the south (Fig. 1). The West Africa - Amazonian Craton underwent amalgamation with other cratonic landmasses along several orogenic belts during the Brasiliano-Pan-African orogeny (ca. 600 Ma). This event culminated in the emergence of the West Gondwana paleocontinent (Buiter and Torsvik, 2014, Cordani et al., 2009). Subsequently, the West Africa - Amazonian Craton experienced disruption through Jurassic to early Cretaceous rifting in the equatorial Atlantic region (Basile et al., 2005). The effects of different periods of

60 Mesozoic extensional tectonics associated with the break-up of the Pangea and Gondwana supercontinents allowed basin formation along the proto-Caribbean margin and into the intracontinental cratonic regions of South America, (~~Fig. 1;~~ Vaz et al., 2007). This rift event ultimately led to the partitioning of the Amazonian and West Africa cratonic counterparts, positioning them in South America and Africa, respectively.
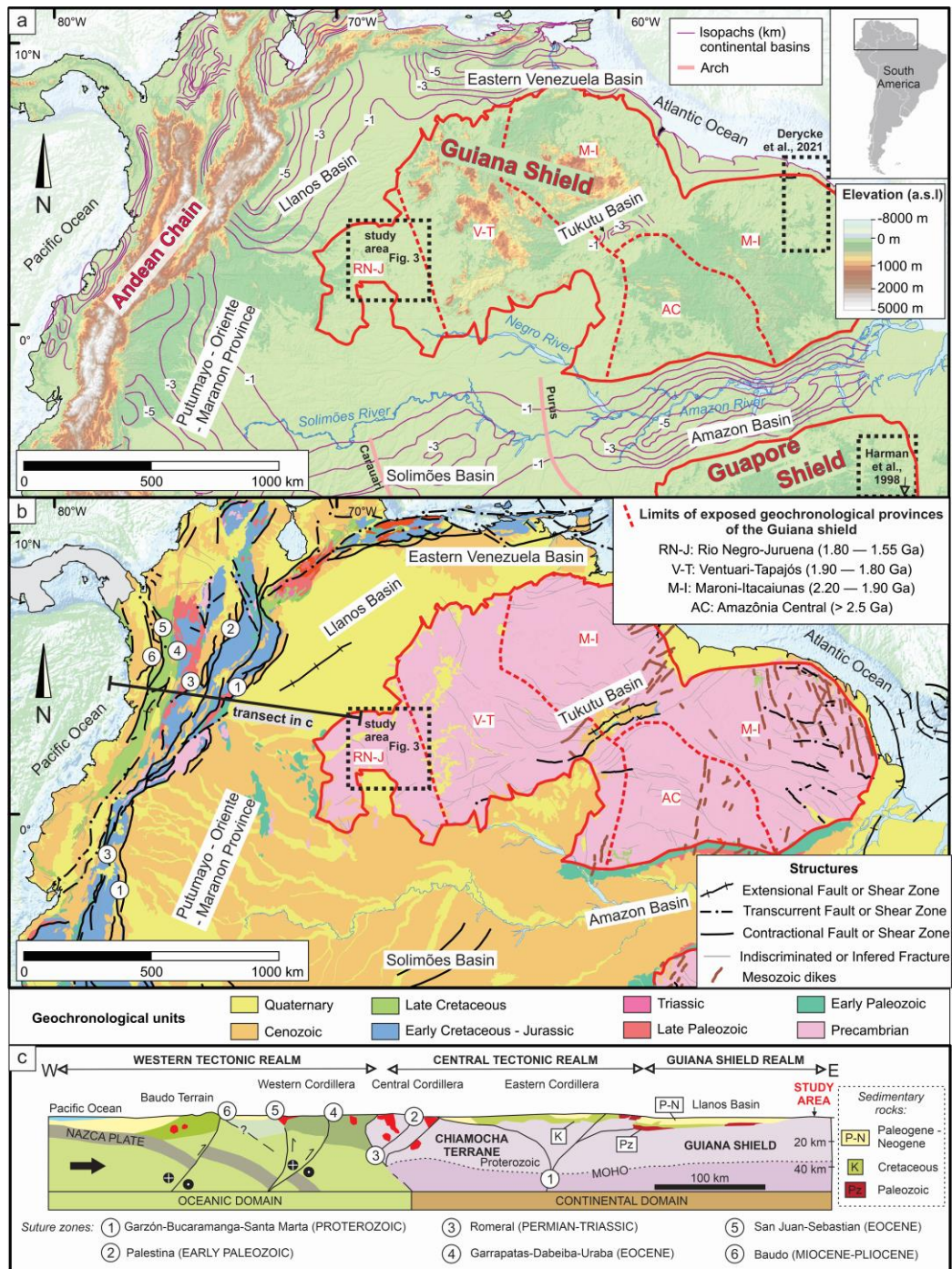
Figure 1: a) Digital elevation map (SRTM, USGS) of northern South America. ~~with main tectonic structures, terranes and basins indicated (modified from Gómez et al., 2019).~~ Our study area and the regions where previous low-temperature thermochronology date were obtained are delineated by the dashed boxes. b) Geochronological units with main tectonic structures, terranes and basins

 c~~b~~) E-W schematic regional structural section across the central region of the Northern Andes into the western Amazonian Craton (Modified from Cediel et al. 2003).

70

The Amazonian Craton is divided into various geochronological domains or provinces, with each exhibiting unique structural and Precambrian geochronological patterns, indicative of different origins for these individual domains. One ~~section among the various different geochronological domains or provinces~~them~~of these~~ ~~constituting the Amazonian Craton~~ is the Rio Negro-Juruena belt, located at the western margin of the craton (Fig. 1). The ~~Rio Negro-Juruena~~ belt ~~is a region with a controversial history, in Colombia,~~ consist~~s~~ing of Paleoproterozoic (1.80-1.50 Ga) gneisses in amphibolite facies and granitoids, and Mesoproterozoic (1.40-1.34 Ga) anorogenic magmatism (Bonilla et al., 2023, 2021; Cordani et al., 2016; Tassinari and Macambira, 1999; Teixeira et al., 1989~~; Tassinari and Macambira, 1999; Cordani et al., 2016; Bonilla et al., 2021, 2023~~). During the Jurassic to the early Cretaceous, the belt delimited the Llanos and Putumayo-Oriente-Maranon basins that were evolving as a back-arc rifting zone (Fig. 1; Guerrero et al., 2020; Cediel and Shaw, 2019; Horton, 2018~~; Cediel and Shaw, 2019; Guerrero et al., 2020~~). The Rio Negro-Juruena belt has been investigated with several geochronometers such as zircon U-Pb, whole rock Sm-Nd, whole-rock Rb-Sr and mica K-Ar (Bonilla et al., 2023~~1~~, 2021~~3~~; Cordani et al., 2016; Santos et al., 2000; Tassinari and Macambira, 1999)~~.,~~ ~~but~~ However, only one sample ~~study involved~~was ~~dated~~analyzed using a low-temperature thermochronology technique. ~~As as a~~apatite fission track analysis for the one sample yielded ~~thermochronology~~ ~~(with~~ a central age of ca. 180 Ma~~)~~, leading to only a limited preliminary correlation between Mesozoic exhumation and extensional tectonics in the region (Bonilla et al., 2020). Nevertheless, the application of these techniques can enrich our understanding of the more recent evolution of craton evolution and (in)stability (Kohn and Gleadow, 2019). Furthermore, the gathered thermochronological data has the potential to yield significant tectonic insights on the evolution of craton-adjacent sedimentary basins (e.g. Guerrero et al., 2020; Hurtado et al., 2018; Vallejo et al., 2017; Horton et al., 2010~~; Hurtado et al., 2018; Vallejo et al., 2017~~). Up to the present, low temperature thermochronology studies in northern South America were mainly directed towards the Andean orogen (e.g. Pérez-Consuegra et al., 2021; Amaya et al., 2017; Villagómez and Spikings, 2013; Villagómez et al., 2011; Parra et al., 2009; ~~Pérez-Consuegra et al., 2021;~~ Spikings et al., 2000~~; Villagómez et al., 2011; Villagómez and Spikings, 2013~~). This study specifically aims at filling part of this gap and reconstructing the thermal history of the large and under-explored cratonic Guiana Shield, with implications for gaining deeper insights into the evolution of some of the most prominent Colombian sedimentary basins. We analysed 20 crystalline basement samples with apatite fission track (AFT) thermochronology in order to reconstruct the thermal history of the basement rocks from the Rio Negro-Juruena belt of the western Guiana Shield. Additionally, we compare our findings with prior thermochronological research of cratonic areas that once composed West Gondwana to gain insights into the mechanisms underlying Phanerozoic craton destabilizing processes.
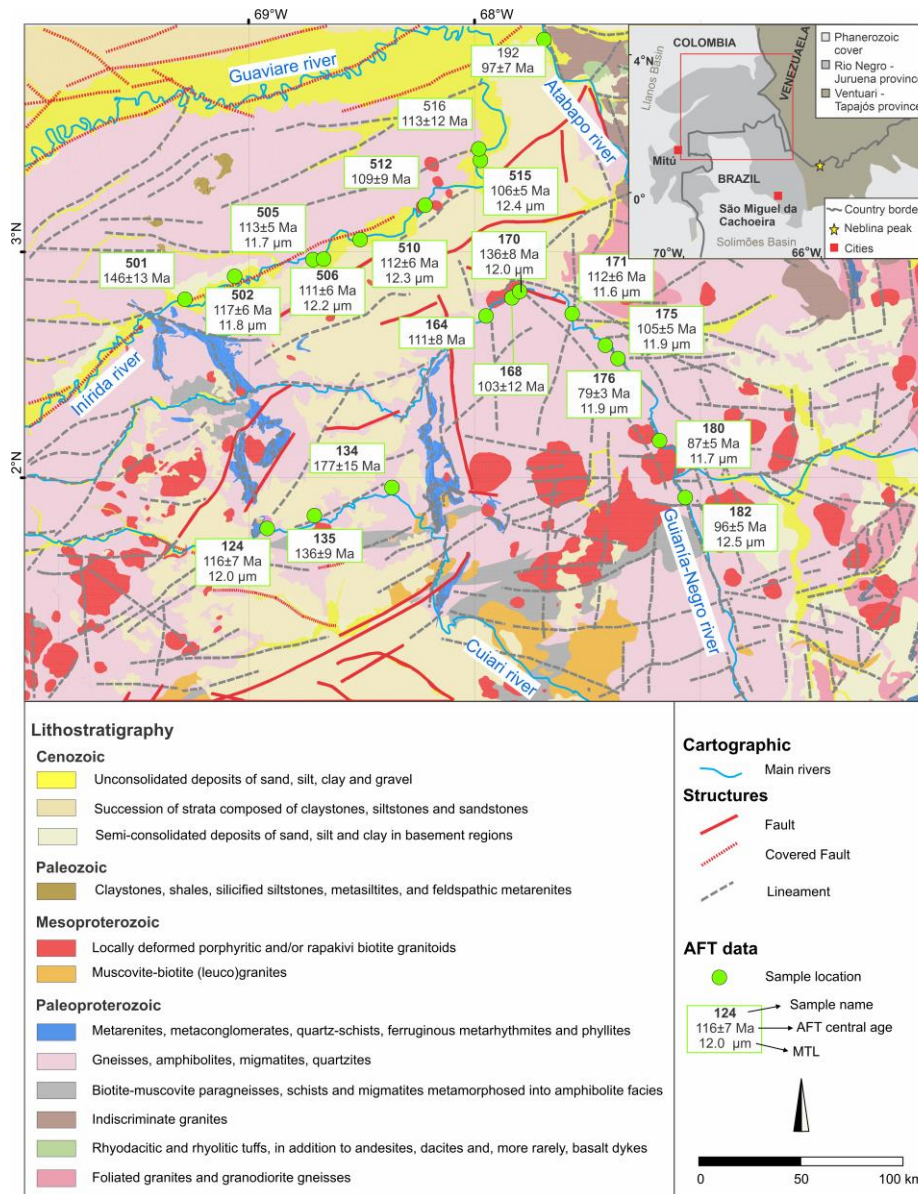
Figure 23: Geological map of the study area with sample site locations and apatite fission track (AFT) results (modified from Almeida and Mendes, 2021).

2 Geological Setting

During the Proterozoic, the Amazonian–West Africa Craton further amalgamated with the development of accretionary orogenic belts along the western margin of its Archean nucleus, named the Amazonia Central province (> 2.5 Ga; Santos et al., 2006; Tassinari and Macambira, 1999; Santos et al., 2006). These belts are referred to as the Maroni-Itacaiunas (ca. 2.20 –

1.90 Ga) Ventuari-Tapajós (ca. 1.2.90 - 1.8 Ga), Rio Negro-Juruena (ca. 1.8 – 1.55 Ga), Rondonian-San Ignacio (ca. 1.5-1.3 Ga), and Putumayo (1.45–0.98 Ga) belts. Their formation ages decrease towards the current Andean margin of South America (Fig. 1; Cordani and Teixeira, 2007; Ibanez-Mejia et al., 2011; Cordani and Teixeira, 2007; Tassinari and Macambira, 1999). Our study area comprises the NW sector of the Amazonian Craton, in the Rio Negro-Juruena belt, near the projected suture

110 with the Ventuari–Tapajós belt (Fig.1), as traced by Cordani and Teixeira (2007). The area includes the boundary between Colombia with Venezuela and Brazil (Fig. 23), where the geology has remained relatively unexplored due to the challenges posed by limited accessibility, the absence of road infrastructure, and extensive vegetation cover. In the western and north direction, towards the Andes and Venezuela, and in the southward direction, towards the Amazon River, the Precambrian basement is buried under a thick sedimentary cover of the Llanos and Putumayo-Oriente-Maranon basins, which has a record

115 at least since the Paleozoic (Fig. 1) (Moreno-López and Escalona, 2015). Here, we provide a concise overview of the tectonic evolution of the research area. For more complete information, we recommend, amongst others, the publications by Cediel and Shaw (2019) and Bonilla et al. (2021) and references therein.

2.1 Precambrian

120 The basement rocks of the Rio Negro-Juruena belt in Colombia (Fig. 2) the study area encompass Paleoproterozoic to Mesoproterozoic (1.805 – 1.550 Ga) (meta)granitoid rocks, mostly calc-alkaline gneisses, granites, and migmatites that experienced amphibolite facies metamorphism (Fig.3; Bonilla et al., 2021; Cordani et al., 2016). Based on available Rb-Sr and Sm-Nd data, these rocks are thought to have originated from a sequence of Proterozoic subduction events involving juvenile magmatic arcs (Cordani et al., 2016; Tassinari and Macambira, 1999; Cordani et al., 2016). Some areas contain low-grade

125 metamorphosed volcanic-sedimentary sequences and intraplate Mesoproterozoic anorogenic granites (Fig. 23). K-Ar dating on micas of these rocks indicates a widespread intraplate heating event, with basement temperatures exceeding 300°C around 1.2 – 1.3 Ga (Cordani et al., 2016). The thermal event was constrained by U-Pb apatite ages and it has been related to large anorogenic magmatism in a continental rift (Bonilla et al., 2023)

The Amazonian-West Africa Craton became part of the Rodinia supercontinent around 1.0 Ga ago through a continental

130 collision of its western margin with southern Laurentia (Ibanez-Mejia et al., 2011; Li et al., 2008; Kroonenberg, 1982; Ibanez-Mejia et al., 2011; Li et al., 2008), while during the Neoproterozoic (ca. 700-600 Ma), break-up of Rodinia separated them again (Li et al., 2008; Cawood and Pisarevsky, 2006). In the late Neoproterozoic (ca. 600-500 Ma), the margins of the Amazonian-West Africa craton collided with the eastern South American and African cratons, along suturing orogenic belts, eventually resulting in the formation of West Gondwana (Johansson, 2014; Li et al., 2008).

135 ## 2.2 Phanerozoic

For the entire Paleozoic, more specifically from the late Neoproterozoic to the early Mesozoic, the Amazonian-West Africa craton was part of the continental interior of Gondwana and Pangea. It remained at the hinterland of the palaeocontinents until

their break-up. Early Mesozoic rifting affected both sides of the study region. On the western margin of northwestern Gondwana, arc magmatism and marine incursions occurred during a prevailing extensional regime (Spikings et al., 2019; Cardona et al., 2010). The current Andean orogenic cycle started during the Jurassic, following a pause in subduction between the late Permian and late Triassic (Ramos and Aleman, 2000). Since then, oceanic subduction has been continuous (Pankhurst et al., 2000; Coira et al., 1982; James, 1971). During the Jurassic and Cretaceous, the northern Andean margin was characterized by the development of a prominent volcanic arc with back-arc extension (Spikings et al., 2015; Maloney et al., 2013; Horton et al., 2010). The Putumayo-Oriente-Maranon Province and Llanos basins (Fig. 1) experienced rifting and tectonic subsidence due to this back-arc extension (Horton et al., 2010; Parra et al., 2009; Horton et al., 2010), accumulating primarily Cretaceous shales and marls within a shallow marine environment (Fig. 32; Jiménez et al., 2020; Villamil and Arango, 1998; Cooper et al., 1995). Occasionally, sandstone and limestone units prograde locally. In general, during the Aptian-Albian (ca. 120 – 100 Ma), the deposits accumulated in continental and shallow-marine to tidal environments, while the Cenomanian-Coniacian (ca. 100 – 85 Ma) strata were predominantly formed in a deeper marine, shelf environment (Fig. 32; Villamil and Arango, 1998; Cooper et al., 1995). Albian magmatism (ca. 103 Ma) is recorded in the Colombian basement in the continental interior (Ibañez–Mejia et al., 2014). A Santonian-Maastrichtian (ca. 85 – 65 Ma) regressive sequence comprises deposits from both marine and coastal plain settings (Fig. 32). Marine deposition was abruptly terminated during the early Maastrichtian (ca. 70 Ma) due to the accretion of the Western Cordillera that also uplifted the basin area in the hinterland (Fig. 32; Cooper et al., 1995). From the early Cenozoic to the present (ca. 70 – 0 Ma), the Putumayo and Llanos basins acted as foreland basins, subsiding due to the orogenic load of the Andean terrains.

Meanwhile, in the equatorial Atlantic passive margin between northern South America and western Africa (Sapin et al., 2016; Deckart and Gilbert, 1997) incipient rifting is thought to have started in the early Jurassic, coinciding with significant volcanic activity documented in the Central Atlantic Magmatic Province ca. 200 Ma ago (CAMP; Marzoli et al., 2018; Marzoli et al., 1999). In the Cretaceous, the extension ultimately transpired through transpressional and transtensional deformation until the complete rupture of the paleocontinent in the Aptian (ca. 120 Ma) and consequential opening of the Atlantic Ocean. This rupture resulted in the effective separation of the Amazonian and West Africa cratons, which became situated within South America and Africa, respectively.

In the interior of the Amazonian craton, the Takutu rift basin (Fig. 1) evolved as an aulacogen related to the opening of the equatorial Atlantic Ocean (Vaz et al., 2007). Triassic tholeiitic dykes from the CAMP and early Cretaceous flood basalts with ages of ca. 140 Ma intruded the Takutu rift basement (Reis et al., 2006). Moreover, alkaline nepheline-bearing syenites of 111 ± 1 Ma and 116 ± 3 Ma are found in the surrounding basement adjacent to the basin (Figueredo et al., 2018). Sedimentation in the Takutu rift basin occurred between the early Jurassic and the early Cretaceous (Sapin et al., 2016). The deposits have an estimated thickness of around 7300 meters, encompassing continental volcanic-sedimentary sequences (Vaz et al., 2007). The clastic basin fill includes alluvial to lacustrine conglomerate, sandstone, claystone, and shale (Sapin et al., 2016).
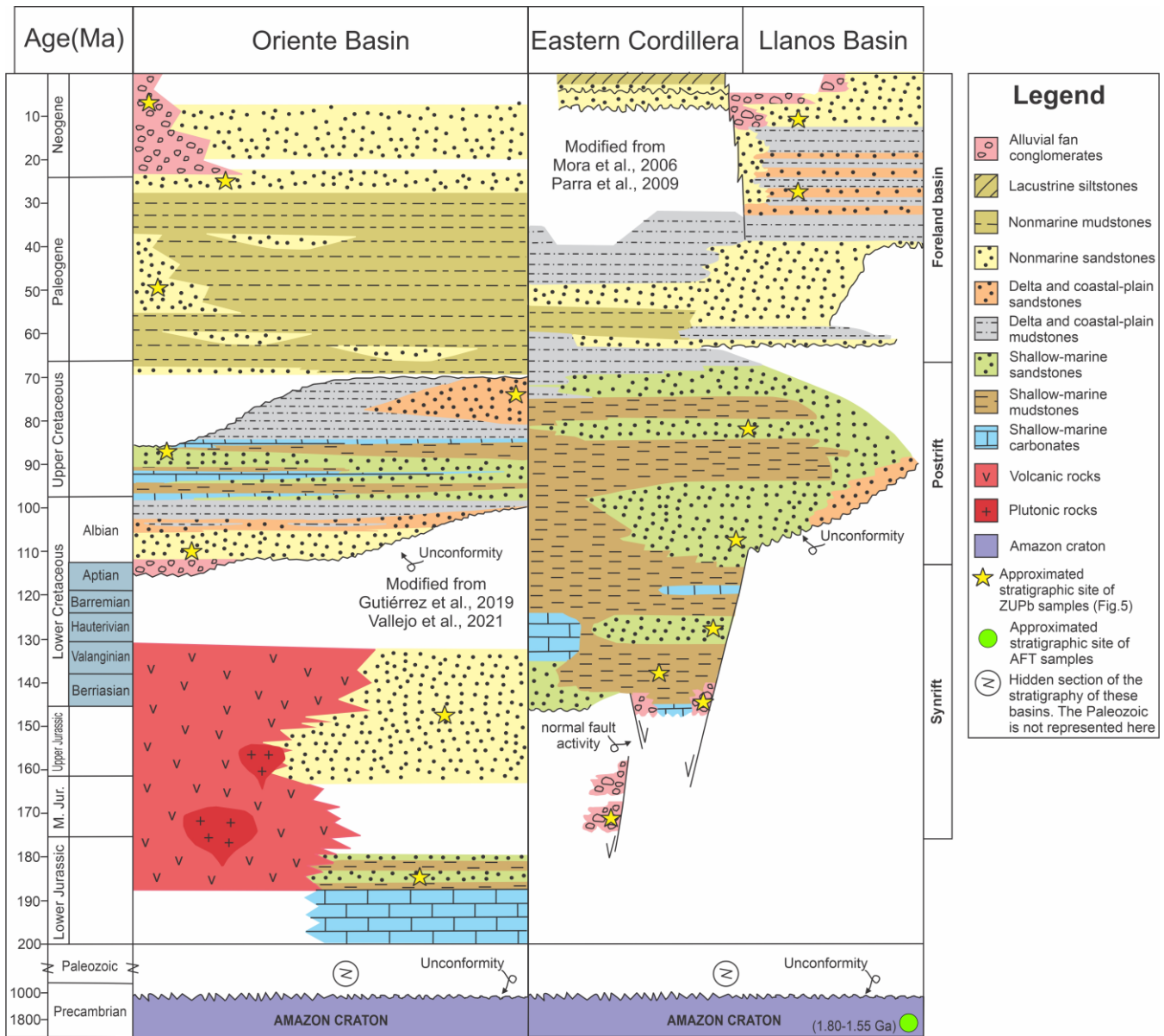
Figure 32: Simplified stratigraphic chart of the Llanos and Oriente basins providing the stratigraphic context for published detrital zircon U-Pb data that we depict in Fig. 65 (modified from Mora et al. 2006; Parra et al., 2009; Guitiérrez et al., 2019; Vallejo et al., 2021). The ages in blue refer to the time range of basement cooling constrained by our AFT data.

3 Samples and methods

Samples were taken from outcrops of the Rio Negro - Juruena belt along one NNW-SSE, and three ENE-WSW oriented profiles along the Guainía-Negro, Inírida and Cuiari rivers (Table 1; Fig. 1 and 3). Previously obtained zircon and apatite U-Pb (ZUPb-APUPb) ages for these samples indicate that they were all formed between 1.85 and 1.50 Ga, except for sample

502, which had a slightly younger weighted mean ZUPb age of 1.40 Ga (Bonilla et al., 2021). A regional Mesoproterozoic thermal event results in the reseating of APUPb ~ 1.40 Ga (Bonilla et al., 2023).

180   The apatite fission-track (AFT) method was used to reconstruct the thermo-tectonic evolution of the belt. The AFT method is based on the natural fission decay of ^{238}U which creates lattice damage trails, known as fission tracks, within the apatite crystal. Over time, these fission tracks accumulate at a constant rate, and the number of tracks per unit area serves as a measure of the AFT age. As f~~The f~~ission track ~~dating~~methods in general, and for apatite in particular, ~~is~~are ~~extremely~~ sensitive to low temperatures~~.~~, ~~The~~ an AFT age represents a "cooling age" since fission tracks in apatite beca~~o~~me stable and ~~are~~ retained. This

185   occurs at relatively low temperatures of around 120°C over geological timescales~~temperatures below ca. 120°C~~. This temperature corresponds to a depth of about 4 km in the continental crust, when considering a geothermal gradient of 25-30°C/km. At temperatures higher than ca.120°C, fission tracks in apatite are annealed completely over geological time-scales (e.g., Gleadow and Brown, 2000). Between approximately 120°C and 60°C, fission tracks in apatite are preserved but are shortened due to the thermal restoration of the crystal lattice. This temperature range is known as the apatite partial annealing

190   zone (APAZ; Wagner and Van den haute, 1992 and references therein). Importantly, these temperatures are a simplification of the approximate limits of the APAZ, since multiple studies indicate that these thresholds are affected by the composition of the apatite grain, particularly concerning its chlorine content, and the rock's cooling rate (Green et al., 1985; Gleadow and Duddy, 1981). Despite the~~se~~ complexities, ~~At temperatures higher than ca.120°C, fission tracks in apatite are annealed completely over geological time scales (e.g., Gleadow and Brown, 2000). As a result, t~~the AFT length provides information

195   about the past temperatures experienced by the apatite-bearing rock during its evolution in the Earth's crust (Ketcham et al., 2007; Gleadow et al., 1986~~; Ketcham et al., 2007~~). The annealing behavior and shortening of apatite fission tracks can hence be exploited for thermal history modeling (e.g., Gallagher, 2012; Ketcham, 2005; Laslett et al., 1987).

Sample ID	Latitude (°N)	Longitude (°W)	Lithology	Elevation (m)
124	1.778028	68.917570	Porphyritic syenogranite	154
134	1.959167	68.364610	Monzogranite	135
135	1.834278	68.707450	Quartz monzodiorite	147
164	2.718608	67.948862	Monzogranite	98
168	2.798120	67.834094	Monzogranite	97
170	2.827199	67.799111	Monzogranite	111
171	2.728289	67.567755	Migmatite	88
175	2.589041	67.420448	Leucosome	84
176	2.529057	67.365048	Migmatite	90
180	2.166866	67.181351	Migmatite	86
182	1.914885	67.066977	Monzogranite	81
501	2.792967	69.281958	Syenogranite	133
502	2.893865	69.061838	Monzogranite	128
505	2.967441	68.714423	Quartzsyenite	112
506	2.970117	68.667985	Quartzsyenite	107
510	3.056191	68.506132	Monzogranite	107
512	3.208222	68.218030	Monzogranite	95
515	3.407566	67.973478	Monzogranite	86

| 516 | 3.458146 | 67.981013 | Monzogranite | 93 |

Table 1: Sample locations of the analysed samples in this study, spatially displayed in Fig. 2. Lithology and elevation above sea level is also indicated.

200

In the present work, the AFT analyses were conducted using the external detector (ED) method (Fleischer et al., 1975). All samples were irradiated using one irradiation container in the well-thermalized channel X26 of the BR1 reactor (Belgian Centre for Nuclear Research, SCK, Mol, Belgium). Thermal neutron fluence was monitored using four ED-covered Uranium-doped glass dosimeters IRMM-540R (De Corte et al., 1998), spatially distributed in the irradiation package. Latent fission tracks in

205 apatite were etched using a 5.5M nitric acid solution for 20s at 21°C. Induced fission tracks were revealed in the ED muscovite with 40vol% HF etchant for 40min at 21°C. The Overall Weighted Mean Zeta (OMWZ) based on both Durango (McDowell et al., 2005) and Fish Canyon Tuff (Hurford and Hammerschmidt, 1985) apatite age standards for analyst SN using IRMM-540R glass dosimeters is 286.3 ± 3.9 (1σ) a*cm². The spontaneous and induces fission tracks in both the standards and samples were manually counted using a Nikon Eclipse Ni-E microscope. The microscope was equipped with a DS-Ri2 camera and set

210 to a magnification of 1000x. To facilitate the counting process, the Trackflow software was employed (Van Ranst et al., 2020). The lengths of confined fission tracks and their angles to the c-axis were measured using the same microscope setup. The sub-horizontal confined tracks were corrected for inclination.

4 Results

The AFT results on twenty apatite samples from the Rio Negro-Juruena belt are shown in Table 2 and geographically displayed

215 in Fig. 23. AFT central ages range from 79.1 ± 3.2 Ma to 177.1 ± 14.8 Ma and 14 out of 20 samples yield central ages between 95 Ma and 120 Ma. Where possible, 20 or more apatite grains were analysed per individual sample. Three samples (168, 192 and 506) fail the chi-squared test on 95% confidence level (i.e. $P(\chi^2) < 0.05$). The study area is characterized by large flood plains and rare inselbergs from which most samples were collected, thus only a limited elevation difference (<100m) exists between all samples. Therefore, no age-elevation scatter plots were made. A minimum of 50 confined tracks could be measured

220 for 12 out of 20 samples, and 100 for 9 samples. These samples present uncorrected mean track lengths between 11.6 and 12.5 µm, standard deviations from 1.4 µm to 2.0 µm, and a negatively skewed distribution that is typical from samples with some degree of track annealing. Dpar values range from 1.1 to 1.5 µm, which indicates chlorine-poor apatite. The D_{par} variation seems not to be correlated with the AFT central age (Supplement S3, Fig.S.42).

5 Thermal History Modelling

225 Samples with more than 50 confined track length measurements underwent inverse thermal history modeling using QTQt 5.6.3 (Gallagher, 2012). QTQt uses the transdimensional Markov Chain Monte Carlo search method to find a range of probable time-temperature path solutions (Gallagher, 2012) based on the sample's AFT dataset to reconstruct its thermal history. We

applied 10^5 burn-in and post burn-in iterations. The present-day surface temperature constraint was set as 30 ± 5 °C (CDA, 2020) for all models. The Rio Negro Juruena basement is an area with dense vegetation and few outcrops. There is also limited accessibility for structural and geological observations and absence of Mesozoic sediments. Hence, it was only possible to define reliable constraints to the thermal history models based on the other available geochronology results. For some of the model runs we chose a Mesoproterozoic constraint (1250 ± 50 Ma; 350 ± 50°C) based on the K-Ar and U-Pb apatite dating of the metamorphosed volcanic-sedimentary sequences of the study area (Bonilla et al., 2023; Cordani et al., 2016; Bonilla et al., 2023). Constraints at higher temperatures and further back in time (e.g. the available ZUPb data) would not affect the modeling (Abbey et al., 2023). Details concerning the thermal history modeling and the strategies usedand importance of evaluating acceptance rates are given in Supplement S4.

Initially (modeling strategy M1), we modeled each sample employing the default priors in QTQt (Gallagher, 2012). These priors include a temperature range of 70 ± 70°C and an age range of central age $\pm$ central age. Track length data were converted to c-axis projected lengths (Ketcham et al., 2007a). The multi-kinetic apatite fission track annealing model of Ketcham et al. (2007b) with the etch pit diameter (D_{par}) as kinetic parameter was used. The results for the expected models (Supplement S4, Fig. S.43) indicate a common thermal history for the entire study area. They show a gradual slow cooling through the APAZ (at rates of ca. 0.4°C/Ma) from the Triassic to the late Cretaceous.

One representative sample (sample 171) was chosen to test the variability of these thermal histories in five other modelling strategies (i.e., M2 to M6; Fig. 4). All generated models have demonstrated alignment between the predicted and observed AFT data parameters (Fig. 4). Modeling strategy M2 was performed using the c-axis projection for the track length data and default priors in QTQt. For modeling strategy M3, the priors were widened to 300 ± 300 Ma for time and 150 ± 150°C for temperature. The results obtained from M2 and M3 closely resembled those obtained from modelling strategy M1 in which the expected t,T-path displays a continuous and slow cooling through the APAZ during the Meso-Cenozoic. Acceptance rates for time and temperature and birth and death were however not satisfactory for these strategies (see Supplement S4).

Sample	n	ρ_s (10^6tr/cm²)	N_s	ρ_i (10^6tr/cm²)	N_i	ρ_d (10^6tr/cm²)	N_d	Pooled age ± 1σ (Ma)	Central age ± 1σ (Ma)	P(χ²)	l_m	σ	l_{mc}	σ_c	n_l	D_{par} (µm)
124	25	1.050 (0.033)	984	0.733 (0.028)	702	0.581 (0.008)	5290	115.5 ± 5.9	116.3 ± 6.7	0.22	12.0	1.6	13.6	1.1	71	1.3
134	20	0.762 (0.030)	653	0.342 (0.020)	300	0.581 (0.008)	5623	175.5 ± 12.7	177.1 ± 14.8	0.19	-	-	-	-	-	1.3
135	20	0.729 (0.024)	909	0.430 (0.018)	551	0.581 (0.008)	5159	135.8 ± 7.6	136.4 ± 9.3	0.10	-	-	-	-	-	1.4
164	20	0.394 (0.019)	453	0.283 (0.016)	320	0.553 (0.007)	5624	111.2 ± 8.3	111.2 ± 8.4	0.96	-	-	-	-	-	1.2
168	28	0.296 (0.016)	329	0.242 (0.016)	238	0.557 (0.007)	5688	109.2 ± 9.4	103.4 ± 12.0	0.02	-	-	-	-	-	1.3
170	25	0.554 (0.016)	1147	0.324 (0.012)	673	0.558 (0.007)	5714	134.8 ± 6.8	135.5 ± 7.6	0.22	12.0	1.5	13.5	1.1	65	1.2
171	25	1.040 (0.031)	1101	0.725 (0.026)	778	0.560 (0.007)	5746	112.5 ± 5.5	112.1 ± 6.1	0.20	11.6	2.0	13.4	1.2	100	1.3
175	25	0.754 (0.023)	1060	0.575 (0.020)	803	0.562 (0.007)	5771	105.4 ± 5.1	105.4 ± 5.3	0.73	11.9	1.7	13.3	1.5	100	1.1
176	25	3.050 (0.077)	1570	3.110 (0.078)	1591	0.564 (0.007)	5789	79.1 ± 3.0	79.1 ± 3.2	0.85	11.9	1.7	13.5	1.2	100	1.3
180	25	0.639 (0.019)	1101	0.581 (0.018)	1023	0.572 (0.007)	5830	87.5 ± 4.0	86.6 ± 4.7	0.10	11.7	1.7	13.4	1.0	100	1.5
182	30	0.883 (0.023)	1462	0.746 (0.021)	1256	0.573 (0.008)	5824	94.8 ± 3.9	96.1 ± 4.8	0.07	12.5	1.6	13.9	1.0	100	1.4
192	10	4.320 (0.129)	1114	3.640 (0.120)	919	0.581 (0.008)	5623	100.0 ± 4.7	97.0 ± 7.3	0.00	-	-	-	-	-	1.5
501	25	0.359 (0.018)	405	0.197 (0.013)	225	0.574 (0.008)	5811	146.3 ± 12.3	146.3 ± 12.5	0.78	-	-	-	-	-	1.3
502	25	1.630 (0.044)	1397	1.140 (0.036)	985	0.575 (0.008)	5798	115.7 ± 5.1	116.8 ± 6.3	0.14	11.8	1.6	13.5	1.0	100	1.3
505	20	1.720 (0.042)	1692	1.270 (0.036)	1221	0.576 (0.008)	5783	113.3 ± 4.5	113.3 ± 4.8	0.56	11.7	1.4	13.4	1.1	100	1.4
506	25	2.180 (0.047)	2193	1.670 (0.041)	1634	0.577 (0.008)	5763	109.9 ± 3.9	110.9 ± 5.6	0.00	12.2	1.6	13.7	1.1	100	1.3
510	20	1.490 (0.045)	1092	1.090 (0.038)	804	0.578 (0.008)	5735	111.3 ± 5.4	111.5 ± 6.2	0.24	12.3	1.5	13.8	1.2	100	1.3
512	25	0.307 (0.016)	380	0.235 (0.014)	288	0.580 (0.008)	5509	108.7 ± 8.6	108.7 ± 8.8	0.60	-	-	-	-	-	1.3
515	25	0.858 (0.025)	1184	0.677 (0.022)	922	0.581 (0.008)	5462	105.9 ± 4.9	105.8 ± 5.4	0.22	12.4	1.8	13.8	1.2	85	1.3
516	18	0.348 (0.022)	254	0.250 (0.018)	183	0.581 (0.008)	5404	114.4 ± 11.2	113.1 ± 12.2	0.44	-	-	-	-	-	1.1

Table 2: Apatite fission track data of the analysed samples. The number of analysed grains (n), spontaneous (ρ_s) and induced track density (ρ_i) and induced track density in the IRMM-540R glass dosimeter (ρ_d) with their 1σ uncertainties are given. The number of

255 spontaneous tracks (N_s), induced tracks (N_i) and interpolated value for the glass dosimeter (N_d) are also displayed. The pooled age and central age are expressed in Ma. The p-value for the chi-squared test is also given. The raw mean track length (l_m) and c-axis projected (l_{mc}) mean track length, standard deviation (σ: raw; σ_c: c-axis projected) and number of measured tracks (n_l) from confined track length measurements are indicated. Mean D_{par} values are given. In bold are sample data that were modelled with QTQt.
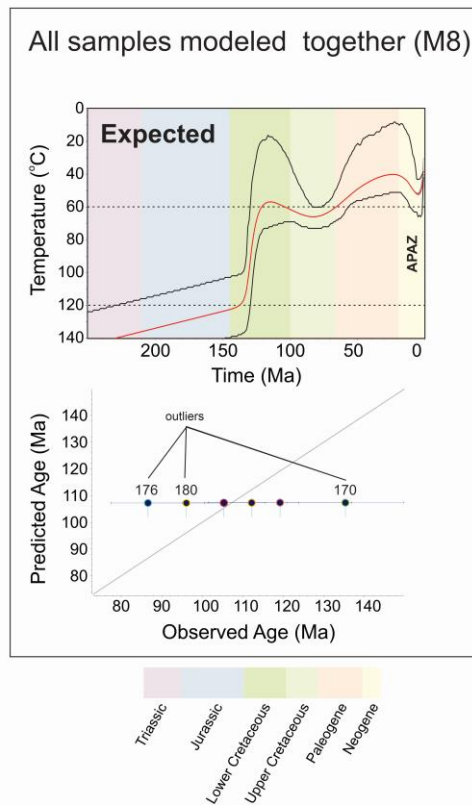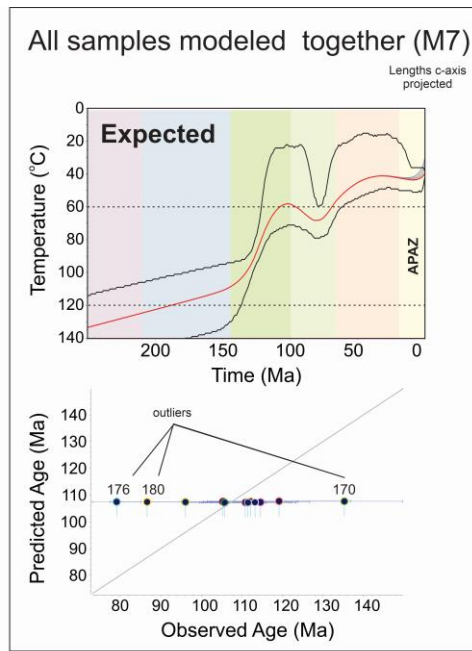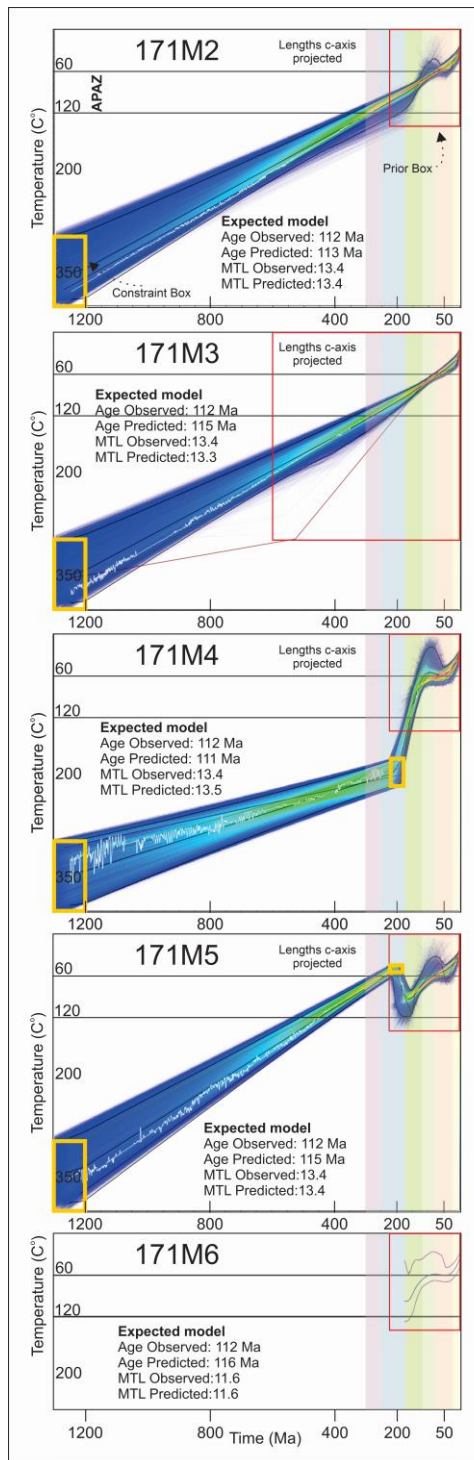
Figure 4: Thermal history modelling results (see section 5 for details).

Modelling strategies M4 and M5 assumed an extra constraint for each model. An artificial zircon fission track age (closure temperature ca. 200°C) equals 200 ± 20 Ma was added for M4 model in order to test the hypotheses of the basement being at

265 temperatures hotter than the APAZ in the early Jurassic. As an opposite hypothesis, an artificial exposure close to surface temperatures in 200 ± 20 Ma was added for M5 model, in this case, the basement would be colder than the APAZ temperatures in the early Jurassic. Interestingly, the expected models, which exhibited a consistent slow cooling trend in the M1, M2, and M3 modeling strategies, showed rapid cooling during the early Cretaceous in both M4 and M5 models. Acceptance rates for time and temperature and birth and death were in addition satisfactory.

270 In modeling strategy M6 we did not use c-axis projected confined track lengths, nor additional constrains. C-axis projection is a commonly employed technique to correct the AFT data for track orientation. It is based on the assumption that confined tracks tend to be longer in directions parallel to the crystallographic c-axis and shorter perpendicular to the c-axis (Ketcham et al., 2007b; Donelick, 199~~9~~1, 199~~1~~9~~; Ketcham et al., 2007b~~). The AFT community has extensively embraced this projection~~correction~~ as the standard length correction. However, our length data deviates from the assumption of angle-length

275 correlation showing no apparent anisotropy in the length distribution (Supplement S2~~3~~). In this case, we decided to also test models without c-axis projection, such as in our M6 modelling protocol, that could be more reliable considering our more isotropic data. The M6 expected model also displays an early Cretaceous rapid cooling through the APAZ. Acceptance rates for time and temperature and birth and death were satisfactory.

Finally, all samples were modeled together in batch modeling strategies M7 and M8. In M7, a c-axis projection was

280 implemented, whereas in M8 not. The results for M7 and M8 were similar. The expected models displayed a fast cooling (at rates of ca. 50°C/Ma) in the early Cretaceous and residence close to the upper APAZ (ca. 60 °C) by the end of late Cretaceous (ca. 65 Ma) followed by slow cooling to surface temperatures. Acceptance rates for time and temperature and birth and death were satisfactory. The majority of the samples exhibited strong alignment between the predicted and observed AFT data parameters, except for samples 176, 180, and 170 (Fig. 4).

285 **6 Discussion**

6.1 Inverse thermal history modeling

The inverse thermal history models (Supplement S4) reveal that the investigated rocks in the Rio Negro-Juruena basement experienced a common cooling history within the APAZ temperature range (ca.120 °C to 60 °C), with no significant differences between samples. Despite the presence of intersecting lineaments suggesting potential faults (Fig. 1 and 3),

290 Phanerozoic fault activity does not seem to have caused substantial differential displacements within the basement samples and this part of the Guiana Shield more or less acted as a single block in response to the Phanerozoic fault activity. Reactivation of faults can induce differential movements and uplift and subsequent erosion, resulting in variations in the rates of cooling. The similarity in paleo crustal depth levels of the exposed Precambrian rocks in the area (Bonilla et al., 2023), along with the

low seismic activity in the region (Pérez-Gussinyé et al., 2009), further supports limited differential younger reactivation of faults during the (Cenozoic). Consequently, the homogeneous rock cooling history observed in the study area aligns well with independent geological evidence, which indicates limited inter-sample reactivation. We acknowledge that samples 176, 180, and 170 seems to exhibit slight deviations from the common cooling trend, as evidenced in the Predicted and Observed ages graph of Model M7 and M8, for instance (Fig. 4). While these variations are notable, pinpointing the precise reasons for these discrepancies remains challenging, given that very distinct thermal histories in these areas lack support from the surrounding outcropping geology or nearby data over small distances in the rather inaccessible area can hitherto not be substantiated due to a lack of outcrop and structural data. Additional sampling and analyses in these areas would hence potentially provide more comprehensive information to validate any differences in thermal history across the entire study area.

The AFT data fits well with two main thermal history model solutions. The first solution is acquired in the M1, M2, and M3 modelling strategy (Supplement S4) and consists of a gradual and continuous cooling process through the APAZ during the Cretaceous, with similar rates persisting until surface temperature conditions are reached as the rocks exhumed. The second solution is acquired in the M4, M5, M6, M7, and M8 modelling approaches and implies a rapid cooling event in the early Cretaceous, specifically between the Berriasian and Aptian (140 – 110 Ma ago), that caused the samples to reach the upper APAZ (ca. 65 °C). This event is followed by a gradual slow cooling to reach surface temperatures. The second solution is supported by four main additional arguments as the most plausible for our data.

The primary argument revolves around the fact that our study area exhibits a common cooling history, which justifies the batch of individual sample data into a one larger dataset as an effective approach for generating more reliable models. Modeling strategies M7 and M8 adopt this approach. The resulting models indicate rapid cooling through the APAZ during the early Cretaceous, representing the second solution. These models have been demonstrated to be well-resolved, showing consistency between the predicted and observed AFT data parameters (see Supplement S4 Fig. 4). Therefore, it appears that M7 and M8 offer reasonable and plausible solutions, supporting the second solution as the preferred one.

The second argument focuses on analysing the maximum likelihood (MaxLike) paths in the M1 models. The MaxLike model represents the time-temperature path that best fits the data. Although in some circumstances it may exhibit a complex and geologically unrealistic solution (Abbey et al., 2023), to our specific dataset, these models generally show straightforward and realistic time-temperature paths. For almost all samples, the MaxLike paths indicated a rapid cooling event from the late Jurassic to the early Cretaceous (see Supplement S4, Fig. S.43). Thus, considering the geologically plausibility of the results and the consistent patterns observed across different samples, it is reasonable to conclude that the MaxLike models, which align with the second solution, provide a reliable indication of the major aspects of the true history provide a credible approximation of the true cooling history.

The third argument stems from the analysis of the modeling results when additional constraints are applied. By incorporating different time-temperature constraints in the modeling strategies M4 and M5, a similar accelerated cooling trend during the Cretaceous is observed for both strategies (Supplement S4). This indicates that the presented cooling event is not significantly affected by the inclusion of potentially new thermochronological or geological information from the past thermal history. In

other terms, regardless of whether the dated rocks were deep in the crust or near the surface in the Jurassic, Cretaceous cooling, i.e., the second solution, is required to align with our data.

330 Finally, applying c-axis correction seems to be inadequate for the data, as discussed in section 5. Consequently, modeling strategies that exclude this correction tend to avoid overcorrections. Both the M6 and M8 models, which don't include the c-axis projection, show a rapid cooling trend in the early Cretaceous, in line with the second solution we discussed. This indicates that the M6 and M8 models support to considering the second solution as the preferred choice.

In conclusion, our AFT data provides strong evidence for a significant rapid cooling event during the early Cretaceous in the

335 Rio Negro-Juruena belt. Out of all the models that favoured this solution, Model M8 is selected for subsequent discussions (Fig. 54).

6.2 Early Cretaceous cooling (140 – 110 Ma)

The early Cretaceous cooling event constrained by our data is most likely a result of the exhumation of the Rio Negro-Juruena

340 belt due to regional denudation. We ruled out the thermal effects of the CAMP plume as the cause of the observed cooling event due to two compelling reasons. Firstly because, the plume's influence in the crust is estimated to have ended ca. 200 Ma ago (Davies et al., 2017), which predates the cooling event constrained by our models (Fig. 54). Secondly, when examining previous data from regions impacted by mantle plumes, there is little to no evidence of the influence of plume impingement in the AFT system, even at relatively close distances (e.g., Sahu et al., 2013; Fonseca et al., 2020), which indicates that the crustal

345 heating resulted from the plume probably is very limited in the upper crust. Therefore, the early Cretaceous cooling event is most likely attributed to the erosion of the upper crust with the subsequent deposition of the produced clastic sediments in adjacent basins, leading to the exhumation of the craton as it appears today.
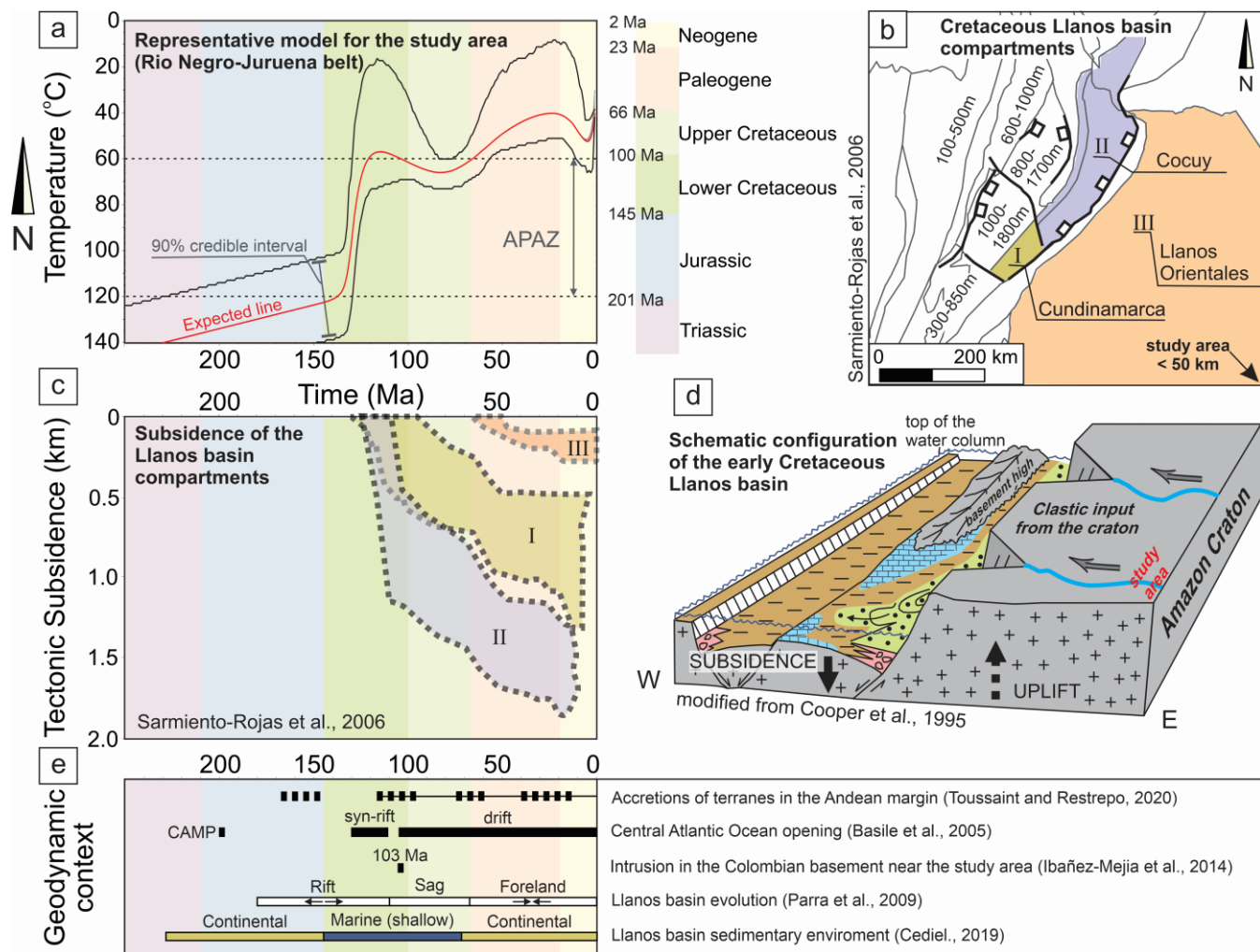
Figure 54: a) Thermal history model derived from the modelling strategy M8 (see Supplement S4), which was chosen as the representative for the study area (section 6.1). **b)** Schematic map of the tectonic compartments of the Llanos Basin during the Cretaceous and their tectonic subsidence in meters (from Sarmiento-Rojas et al., 2006). **c)** The tectonic subsidence of the Cundinamarca (A), Cocuy (B), and Llanos Orientales (C) compartments of the basin (from Sarmiento-Rojas et al., 2006). **d)** Block diagram illustrating the configuration of the Llanos Basin in the early Cretaceous (modified from Cooper et al., 1995). **e)** Main geodynamic events affecting northern South America in the Mesozoic and Cenozoic. CAMP: Central Atlantic Magmatic Province.

In the early Cretaceous, the northwestern margin of South America was evolving in ~~a back-arc~~ extensional settings, marked by the formation of the rifts of the equatorial Atlantic ocean and back-arc rifts from the Andean collision zone ~~-~~(Fig. 54; León et al., 2019; Zapata et al., 2019; Cardona et al., 2010). These back-arc rifts created depocenters in the Llanos Basin and the Putumayo-Oriente-Maranon sedimentary Province (Fig. 1), where early Cretaceous marine sediments started to accumulated over the Jurassic volcanic and siliciclastic units (Fig. 32; Kammer and Sánchez, 2006; Sarmiento-Rojas et al., 2006).

It cannot be ruled out that p~~While the presence of surrounding e~~otential early Cretaceous extensional tectonics, originating from the equatorial Atlantic, ~~during the early Cretaceous, potentially originating from the equatorial Atlantic,~~ may have contributed to ~~stimulating~~invoking tectonic activity and subsequent exhumation within the Rio Negro-Juruena belt. However, ~~, w~~it seems more plausible to attribute~~e attribute~~ the observed exhumation in our study to ~~the~~ extension from the Andean side ~~as the most robust explanation~~. Several key arguments substantiate this interpretation.~~-~~ Firstly, the ~~noteworthy~~ proximity of our study area (less than 100 km) to the Llanos and Putumayo-Oriente-Maranon rift system, compared to the distant Atlantic rift (over 800 km)~~, holds significance~~. In narrow rift~~ing~~ settings such as the incipient equatorial Atlantic, ~~proximity to the rift zone is relevant, as these settings tend to confine~~ deformation seems to be more confined to localized areas without significant deformation ~~over~~reaching greater distances (Sapin et al., 2021). Secondly, the ~~greater~~ alignment between extensional strain directions from the Andean margin and the craton structures likely facilitated the stress reaching our study area. These ~~compelling~~observations ~~aspects~~ thus suggest that the back-arc extension originating from the Andean side ~~acted~~constituted~~ as~~ the primary force driving the exhumation processes in our study area.

Provenance analysis, including petrography and detrital zircon geochronology from the Llanos ~~Basin~~ and the Putumayo-Oriente-Maranon Basin ~~various localities~~ (Guerrero et al., 2020; Guitiérrez et al., 2019; Vallejo et al., 2019~~; Guerrero et al., 2020~~), suggests that ~~before the early Cretaceous~~during the Jurassic, sediments from these basins were mainly sourced ~~by~~from Paleozoic igneous and metamorphic rocks from the Andean basement, located at the western margin of the basins (Fig. 6~~5~~; Hurtado et al., 2018; Horton et al., 2010; ~~Hurtado et al., 2018;~~ Cardona et al., 2010). Detrital zircon U-Pb analysis, however, reveals that Paleozoic sources from the Andean basement disappear, show a systematic decrease in Grenville-aged basement detritus, and a corresponding increase in Paleoproterozoic basement signatures that are only found in the eastern parts of the Guyana shield, including the Rio Negro-Juruena basement (Fig. 6~~5~~; Horton et al., 2010). The provenance analysis confirms that during the early Cretaceous, ~~either~~ the basement rocks of the Rio Negro-Juruena belt or its sedimentary cover~~s~~ previously supplied by this belt experienced erosion~~The provenance analysis confirms that the Rio Negro-Juruena belt experienced erosion during the early Cretaceous and the detrital sediments resulting from the erosion were deposited in the aforementioned depocenters~~. Moreover, the change in the source area that occurred at the Jurassic-Cretaceous boundary suggests tectonic reorganization of the area during that time (Hurtado et al., 2018).

Our interpretation suggests that during the Jurassic, our study area could be characterized by a low-elevation plain, resulting in exceptionally low erosion rates and limited sediment production from the Rio Negro-Juruena basement to the Llanos ~~Basin~~ and the Putumayo-Oriente-Maranon~~adjacent~~ basins (Horton, 2018). Although no ~~preserved~~remnants ~~exist~~are preserved, it is ~~plausible~~possible that ~~either a portion or the entirety of~~ the study area was once, partially or entirely, overlain by Paleozoic sedimentary deposits. This idea is supported by the existence of pre-cretaceous basemen-highs and sedimentary basins to the north and west of the study area (e.g.~~.~~, Arauca Graben, Chiribiquéte sub-basin). This suggests that part of the basement in our study area was buried or not exposed. In the early Cretaceous, tectonic activity intensified, driven by the movement along normal faults of the rifts, which produced kilometer-scale displacements. During this time, the Llanos Basin experienced notably higher rates of tectonic subsidence, providing evidence for increased tectonism (Sarmiento-Rojas et al., 2006). At the

395 upper end of these large normal faults, kilometer-scale tectonic uplift of rifts shoulders and surface topography may have been generated (Buiter et al., 2023). Although in another tectonic setting, it can be similar to the case of the East African Rift System, where border faults create a topographic relief up to two kilometers at the edges of the Tanzania Craton (Ebinger and Scholz, 2011; Corti, 2009, Ebinger and Scholz, 2011).

Another recent parallel can be drawn from the Colorado Plateau within the context of the Basin and Range province in the
400 United States. Much like other rifts, the Basin and Range province is bordered by elevated margins, such as the Sierra Nevada on the western side and the Rocky Mountains along with the Colorado Plateau on the eastern flank (Karl et al., 2022; Heitmann et al., 2021; Rønnevik et al., 2017; Murray et al., 2016; Parsons et al., 2006). The Colorado Plateau stands as a less deformed section of a thick lithosphere, elevated ca. 1.9 km. While there little consensus on the mechanisms behind the plateau uplift (Ding et al., 2022; Tong et al., 2022; Yang et al., 2022; Flowers et al., 2010), thermochronological data suggests that the
405 elevation increase correlated with regional extensional tectonism in adjacent areas (Quigley et al., 2010). We propose that the Rio Negro-Juruena belt likely experienced a similar uplift due to events of tectonic activation of normal faults. This tectonism created a rift shoulder and an elevated plateau that was rapidly eroded by the increased river erosion power (Fig. 54). The fluvial systems transported the detrital sediments to the Llanos Basin and the Putumayo-Oriente-Maranon sedimentary Province, ultimately resulting in the exhumational cooling of the cratonic area observed in our AFT data (Fig. 54).

410 The thermal history modeling indicates a gradual decrease in basement cooling rates in the study area from the late Cretaceous onwards (Fig. 65). Simultaneously, the tectonic subsidence rate of the basins experienced a significant reduction in the post-Cenomanian (post-95 Ma), suggesting a correlation between the decrease in extensional tectonic activity and the diminishing of exhumation rates and sediment production (Fig. 54; Cooper et al., 1995). The subsidence mechanism changed at this time from fault-induced subsidence to thermal subsidence (Sarmiento-Rojas et al., 2006). Our interpretation suggests that the
415 thermal subsidence process during the post-rift phase resulted in a less elevated Rio Negro-Juruena basement in the late Cretaceous compared to the early Cretaceous. The activity of normal faults, responsible for the uplift, had already ceased. This, in turn, led to a reduction in erosion/denudation and thus exhumation rates.
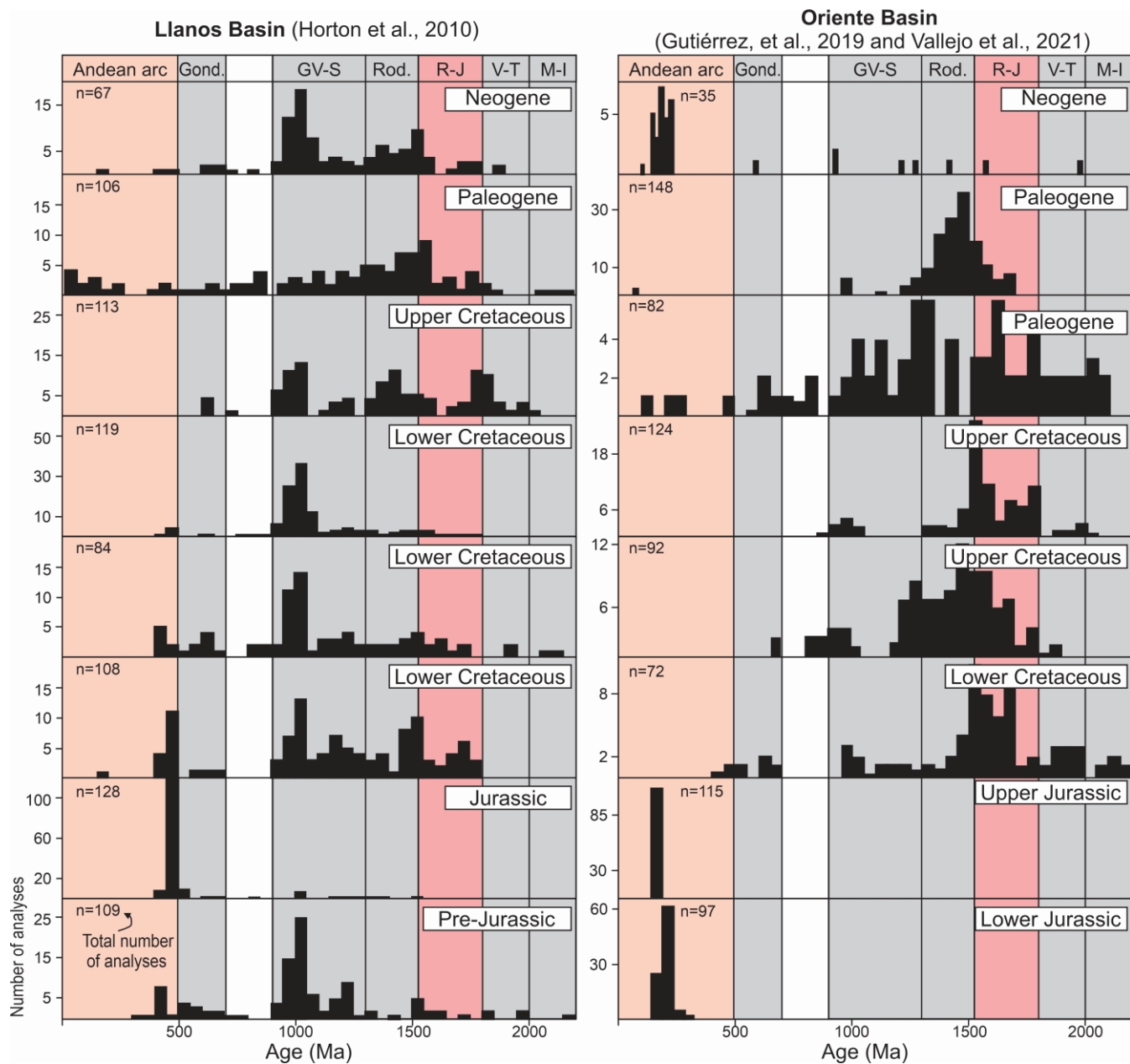
Figure 65: Age histograms depicting detrital zircon U-Pb ages for representative sedimentary rocks from the Llanos and Oriente basins. Stratigraphic location of samples shown in Fig. 3. Data from Horton et al., (2010), Guitiérrez et al., (2019) and Vallejo et al., (2021). M-I: Maroni-Itacaiúnas belt; V-T: Ventuari-Tapajós belt; R-J: Rio Negro-Juruena; Rod.: Rondonia belt; GV-S: Greenville-Sunsás; Gond.: Gondwanides orogeny.

Our data do not reveal evidence of the Cenozoic Andean mountain-building strongly affecting the thermo-tectonic evolution of our study area. The temperature estimates from our samples suggest that they resided in the uppermost crust at in colder conditions, i.e. below the upper APAZ temperature limit (< 60 °C), since the end of the Cretaceous. Thus, there is no significant

thermal overprinting or cooling related to the Cenozoic Andean orogeny in our study area, at least not significant enough to be detectable by the AFT system. This lack of detectable impact might be due to the limitations of the AFT. While our model indicates a mild reheating of about 10 °C around 80 Ma, further investigation is necessary to determine if this event might be real, given the constraints of the AFT method for lower temperatures. ~~Lower temperature t~~Thermochronometers sensitive to lower temperatures, such apatite U-Th/He and monazite fission tracks, would be potential techniques to ~~access~~unveil this event.

In any case, a limited exhumation (ca. 1 km) of the Rio Negro-Juruena belt during the Cenozoic is observed. Detrital sediment provenance data further supports our findings, showing a substantial reduction in the proportion of basement source rocks older than 450 Ma in Paleogene (ca. 66 Ma) and younger deposits (Fig. 6~~5~~; Horton, 2018). Instead, there is a distinct presence of ages characteristic of the late Paleozoic-Cenozoic period (post-300 Ma), which are indicative of Andean sediment sources (Fig. 6~~5~~; Bustamante et al., 2016; Villagómez et al., 2011; Horton et al., 2010~~; Villagómez et al., 2011; Bustamante et al., 2016~~). These Andean signatures are closely linked to Cretaceous-Paleogene magmatic arc rocks and Permian-Jurassic intrusive rocks exposed in the retroarc fold-thrust belt. While direct input from the craton is no longer present, it is worth noting that some recycled cratonic signatures persist in the Paleogene strata. This recycling occurs as old zircon grains are sourced from pre-Andean basin fill within the fold-thrust belt (Horton, 2018; Bande et al., 2012; Horton et al., 2010; Martin-Gombojav and Winkler, 2008~~; Horton et al., 2010; Bande et al., 2012; Horton, 2018~~). The limited contribution of our study area as a sediment source for the surrounding basins, combined with its current low elevation, suggests that the area has likely experienced Cenozoic subsidence instead of uplift. This subsidence could be attributed to the eastward growth of the orogenic wedge that induces regional flexure in the foreland domain. As the sedimentary basins migrated eastward over the craton, the study area probably became part of the distal backbulge zone, leading to a gradual sinking or reduction in elevation over the course of the Cenozoic (Pachón-Parra et al., 2020; Horton, 2018~~; Pachón Parra et al., 2020~~). This resulted in lower erosion and exhumation rates of the craton at that time.

6.3 Comparative analysis across West Gondwana cratonic segments

Based on the concept of cratonic stability, it would be logical to anticipate an ongoing, gradual process of craton exhumation persisting from the Archean or Proterozoic consolidation until the present time. Such an expectation would predict a shared and comparable exhumation history of cratons, consequently leading to comparable results from apatite fission track (AFT) analyses. However, our study, in conjunction with existing research, reveals that this assumption does not hold true. For instance, Green et al., (2022) present a review showing that histories involving long-term slow cooling/denudation may not be appropriate ~~for several supposedly tectonically inactive regions,~~to explain the exhumation of supposedly tectonic inactive regions, such as cratons. Instead, it seems that in many cases, there are repeated cycles of burial and exposure, or heating and cooling, rather than just long-term gradual cooling. Here, we present a brief comparative analysis of AFT data from the Ro Negro-Juruena belt with corresponding data from other cratonic blocks that were once integral parts of the West Gondwana

paleocontinent, specifically the São Francisco Craton (SFC), Rio de la Plata Craton (RPC), West African Craton (WAC), Zimbabwe and Kaapvaal Cratons (ZKC), and Tanzania Craton (TC) (Fig. 7̶6).
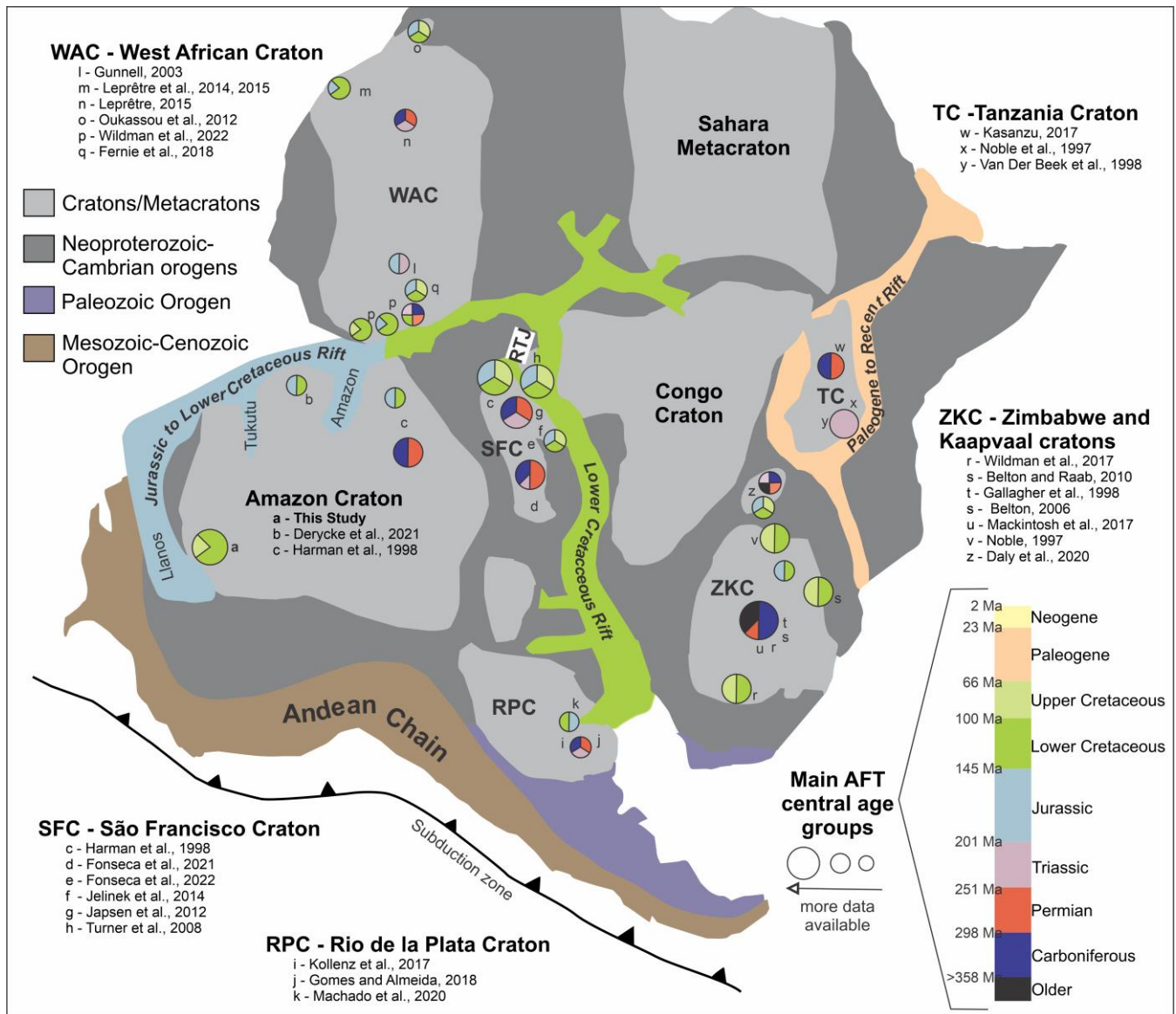
Figure 7̶6: Apatite fission track (AFT) age compilation for cratonic segments that once were part of West Gondwana (ca. 180 Ma). Pie chart size indicates sample quantity, while colours represent main AFT central age groups in the region. RTJ: Recôncavo-Tucano-Jatobá aulacogen.

First we compare our results with those from different regions in the Amazonian Craton. Harman et al. (1998) analysed basement samples along the eastern edge of the Guaporé Shield in Brazil, encompassing the Central Amazonia (> 2.5 Ga) and Maroni-Itacaiúnas (2.2 – 1.95 Ga) provinces (Fig. 1). These samples were categorized into two distinct clusters based on their

460

465

AFT central ages: the first cluster comprises samples yielding Jurassic to Early Cretaceous (ca. 200 – 100 Ma) central ages, while the second cluster consists of samples with central ages from the Permian to the Carboniferous (ca. 310 – 250 Ma) (Fig. 76). The samples from the first cluster were collected along the northern border of the shield and exhibit results similar to ours in terms of AFT central age and mean track length (MTL). In contrast, the samples from the second cluster come from within the interior of the craton. The authors suggest that the differential opening of the equatorial Atlantic Ocean basins was responsible for Meso-Cenozoic exhumation that predominantly impacted the cratonic edge, closer to the rift zones, signifying that proximity to extensional settings influences cratonic exhumation significantly (Fig. 76). Supporting this assumption, AFT results from Derycke et al. (2021) on four samples from the Guiana Shield align well with the first cluster from Harman et al. (1998) as well as our own findings. These samples yield comparable AFT results, i.e., Jurassic to early Cretaceous central ages and medium to long MTL values (ca. 12 µm), suggesting clear Mesozoic cooling. Notably, these samples come from the passive margin of French Guiana, directly influenced by the rifting of the equatorial Atlantic Ocean.

Initial formation of the Takutu rift in the Amazonian Craton is also linked to the opening of the equatorial Atlantic ocean, rendering this region a comparable geological framework (Fig. 1). However, to date, the basement of this rift system has not been analyzed using low-temperature thermochronometric techniques such as AFT, which prevents direct comparisons with our data.

In the context of the opening of the southern Atlantic Ocean in the South America, both the SFC and the RPC underwent a process of rifting, resulting in their separation from their corresponding African counterparts of the Congo Craton and the ZKC (Fig. 76). From the SFC, several AFT studies (Fonseca et al., 2022, 2021; Jelinek et al., 2014; Japsen et al., 2012; Turner et al., 2008; Harman et al., 1998; Turner et al., 2008; Japsen et al., 2012; Jelinek et al., 2014; Fonseca et al., 2021, 2022) consistently show an intricate pattern of craton exhumation (Fig. 76). Central ages spanning the Mesozoic to Cenozoic are particularly concentrated along the borders of the craton, particularly those regions that experienced the effects of Atlantic rifting, specifically along the northeastern borders (Jelinek et al., 2014; Japsen et al., 2012; Turner et al., 2008; Japsen et al., 2012; Jelinek et al., 2014). This age group is also prominent in the vicinity of the Recôncavo-Tucano-Jatobá (RTJ) aulacogen, which evolved during the early Cretaceous (Jelinek et al., 2020). The AFT results suggest that rifting was responsible for km-scale exhumation along the edges of the SFC in the early Cretaceous, potentially through a mechanism akin to the one that triggered the early Cretaceous cooling events in the Amazonian Craton, i.e., a scenario involving the uplift of rift shoulders followed by their subsequent erosion. However, the prevalence of Mesozoic and Cenozoic central ages diminishes significantly as one moves beyond a distance of 50 km from the border rift faults. These younger AFT ages become notably absent, particularly in the more inland portions of the craton, such as in the state of Minas Gerais in Brazil, where the Archean nucleus of the SFC is situated (Fonseca et al., 2021). In these "protected" areas, Paleozoic ages ranging from the Carboniferous to the Triassic prevail, indicating a reduced level of Mesozoic deformation far from the rift zones (Fig. 76). This pattern is also observed in the Harman et al. (1998) study in the Guaporé Shield, where samples from the craton interior also yield Paleozoic central ages. The phenomenon likely stems from the structural rigidity inherent in specific segments of some cratons, effectively channeling deformation into narrow, weakened zones, rather than facilitating its widespread regional propagation.

In our study area, along the western border of the Amazonian Craton, Cretaceous deformation appears to have extended over considerable distances in contrast to observations in the SFC. This is evidenced by the fact that all of our samples, even those from more than 200 km away from the Llanos basin rift show the same thermal history. We hypothesize that the Rio Negro-Juruena belt underwent a reduction in stiffness over its geodynamic history, facilitating and partitioning more widespread

505   deformation during the early Cretaceous rifting. Our suggestion is rooted also in the observation of the comparatively lower elastic thickness of the Rio Negro-Juruena belt, in contrast to other cratonic segments (Pérez-Gussinyé et al., 2007). Much of the geological history of our study area remains elusive, making it challenging to speculate on events that could have potentially influenced lithospheric rigidity. The Mesoproterozoic orogenic events that affected the area stand out as plausible candidates. These events were responsible for generating the extensive NW-SE and NE-SW-trending foliation in the granitic rocks, and

510   were associated with elevated temperatures, reaching amphibolite to granulite conditions (e.g., Mendes et al., 2021).
In southeastern South America, basement samples from the RPC are exposed in a small area (< 400 km^2) along the Uruguayan coast. Rocks from the RPC exhibit a wide spectrum of AFT central ages, i.e. Carboniferous to early Cretaceous (ca. 350 – 100 Ma) (Fig. 7~~6~~; Machado et al., 2020; Gomes and Almeida, 2019; Kollenz et al., 2017~~; Gomes and Almeida, 2019; Machado et al., 2020~~). While there are differing perspectives among these authors regarding the extent to which Mesozoic rifting influenced

515   the craft's exhumation, they collectively concur that the exhumation process was not uniform across the entire cratonic region. It is reasoned that faulting during the Mesozoic might have potentially affected certain distinct cratonic sectors, hence controlling their exhumation and cooling. This observation underscores the ability of the RPC to concentrate deformation in narrow weak zones, similar to the SFC, where a diverse range of AFT ages is localized within relatively small corridors (< 50 km width).

520   In northwestern Africa, the WAC forms the counterpart of the Amazonian Craton (Fig. 7~~6~~). The AFT data obtained from both the southern and northern borders of the craton along the current Atlantic coast closely resemble the AFT results published by Derycke et al. (2021) for samples from the Guiana Shield. The AFT data exhibit early Cretaceous to Jurassic central ages (ca. 200 – 100 Ma) and MTL values of ca. 12 – 13 µm (Oukassou et al., 2012; Fernie et al., 2018; Wildman et al., 2022). The thermal history models unveil episodes of cooling during the early Cretaceous, likely associated with the erosion of rift

525   shoulders resulting from the opening of the Atlantic. Wildman et al. (2022) report a trend of increasing AFT ages with distance from the coast and higher elevation. This phenomenon was attributed by the authors to the specific geomorphology of the passive margin, where the present-day continental drainage divide significantly impacts erosion patterns. Consequently, the greatest denudation magnitudes are found in the region between the coast and the continental divide, leading to older AFT ages within the continental interior (Gallagher and Brown, 1999). However, in instances where the age difference is more

530   pronounced, such as in Benin (Wildman et al., 2019), the elevation difference does not exceed 400 meters. This suggests that the age difference is not solely due to geomorphology and implies that the magnitude of deformation (uplift) has played a role. The extent of this deformation is likely governed by the pre-existing rheology of the craton.
The ZKC, located in the southern part of Africa, stands out as a significantly elevated craton when compared to most other cratonic regions (ca.~~,~~ 1000 meters; Artemieva and Vinnik, 2016). As a general trend, AFT data from the ZKC follow a pattern

similar to the ones previously discussed. Border regions tend to exhibit younger ages, mainly Cretaceous ages (e.g., ; Daly et al., 2020; Wildman et al., 2017; Belton, 2006), while Paleozoic ages are more prevalent toward their centers (e.g., Daly et al., 2020; Mackintosh et al., 2017). Stanley et al. (2013, 2015) and Wildman et al. (2017) proposed that the variable denudation patterns observed in southern Africa, as indicated by AFT data, are likely influenced by a combination of factors. These factors encompass the effects of horizontal plate tectonic stresses at the craton margins, which may have been intensified by changes in plate motions during opening of the South Atlantic Ocean in the Cretaceous, as well as the influence of a lithospheric thermal anomaly. The buoyant upwelling of the mantle could have generated vertical mantle stresses, exerting upward pressure and resulting in the gradual uplift of extensive and robust cratonic interiors. Conversely, areas of weakened lithosphere along the craton margins might have experienced short-wavelength deformations. The ZKC serves as a pertinent case study illustrating that mantle plumes or variations in the mantle dynamics can induce the surface uplift of cratons. Nonetheless, the extent to which this factor significantly triggers exhumation episodes remains uncertain, especially considering the concurrent occurrence of other geodynamic events such as rifting within the same timeframe. In our study area, there is no evidence suggesting that the Central Atlantic Magmatic Province (CAMP) could have triggered a substantial uplift to form an elevated plateau during the Jurassic. Contrarily, the provenance analysis of nearby basins does not indicate the Rio Negro-Juruena belt as a significant source area in the Jurassic (Fig. 65), implying that this area was likely at low elevations during that period.

The TC, located in central Africa, constitutes a relatively small and elevated (>1000 m) cratonic fragment surrounded by high elevated flanks (ca. 1700m) of the East African Rift System (Fig. 76). Tracing its origins back to the Paleogene (35 Ma; Macgregor et al., 2015), the East African Rift System has undergone continuous evolution, manifesting its structural framework through three primary branches. These branches circumvent the Archaean cratons, as the TC, and predominantly propagate through inherited N-striking orogenic belts (Chorowicz, 2005). This context gives us the opportunity to scrutinize the consequences of active intracontinental rifting adjacent to cratons, offering a modern analogue. A rather limited AFT dataset of the TC exists (Kasanzu, 2017; Van Der Beek et al., 1998; Noble et al., 1997; Van Der Beek et al., 1998; Kasanzu, 2017). The central AFT ages in the craton interior are Carboniferous to Permian (ca. 250 – 350 Ma), indicating a limited degree of potential exhumation linked to Cenozoic rifting processes. Nevertheless, the current substantial elevation of the craton suggests that it has probably experienced uplift, yet significant erosion has not yet taken place. At the boundaries with the East African Rift System, basement samples yield Cretaceous AFT ages. These ages are separated from samples with older ages by major faults (Noble et al., 1997). The authors suggest that exhumation was more intense at the TC cratonic margins, which aligns well with our prior observations in other cratons.

In summary, low-temperature thermochronology such as AFT analysis reveals that the exhumation of cratons occurred episodically throughout the Phanerozoic. The process of rifting, particularly during the Mesozoic and Cenozoic disassembly of larger continental units in which the cratons are embedded, has exerted a significant influence on craton exhumation. Exhumation patterns are non-uniform across the cratonic regions, showing variability based on proximity to rift zones or tectonically active boundaries. For instance, in regions such as the SFC and RPC, Mesozoic and Cenozoic ages are clearly concentrated along the craton's borders, especially in areas impacted by Atlantic rifting. In our study area, more widespread

Cretaceous exhumation to within the craton's interior is evident. This can most likely be attributed to the weakening of that
570   specific segment of the cratonic lithosphere. In line with the hypothesis proposed by Bedle et al. (2021), our study underscores the significant role the geological history of the craton and surrounding areas plays in shaping deformation patterns. Events like orogenesis, lithospheric thermal anomalies, and previous tectonic processes can all influence the rigidity and susceptibility of the lithosphere to deformation, ultimately governing the outcomes of the exhumation process.

6 Conclusions

575   This study unveils that the Rio Negro-Juruena belt, situated in the western Guiana Shield (Amazonian Craton) of Colombia, experienced a rapid exhumation event during the early Cretaceous. The AFT central ages range from 79.1 ± 3.2 Ma to 177.1 ± 14.8 Ma with mean track lengths are around 12 µm. The preferred inverse thermal modeling indicates a fast cooling event in the early Cretaceous, result of basement exhumation. This exhumation occurred within a larger context of extensional tectonics, characterized by the presence of Andean subduction related back-arc rifts in the Llanos Basin and the Putumayo-
580   Oriente-Maranon sedimentary Province. Published provenance analyses of sediments from these basins provide compelling evidence supporting the hypothesis that the Rio Negro-Juruena belt served as a significant sediment source during the early Cretaceous. Our interpretation suggests that the tectonic activity associated with the back-arc rifts uplifted the study area, enhancing erosion and ultimately leading to the denudational exhumation of the region.

Moving into the late Cretaceous, the tectonic environment shifted from an extensional to a contractional setting. Basement
585   cooling rates of the Rio Negro-Juruena belt notably decreased, accompanied by diminishing of subsidence patterns in the basins. These changes indicate a decline in tectonic activity in the area, resulting in a reduction in the exhumation of the Rio Negro-Juruena belt. Throughout the Cenozoic, the Rio Negro-Juruena belt likely experienced gradual subsidence and elevation reduction due to the regional flexure induced by the Andean orogeny.

As in our study area, other cratons have been episodically exhumed~~ated~~ during the Phanerozoic. Low temperature
590   thermochronology, especially apatite fission track (AFT) analysis, demonstrates that extensional settings associated with rifting of the continental crust can induce events of surface uplift and subsequent erosion. This process results in the exhumation of deeper parts of the cratons. Mesozoic exhumation episodes are preferentially located along the cratonic rifted borders and/or aulacogens (e.g., Recôncavo-Tucano-Jatobá aulacogen, Brazil). The tectonism does not seems to propagate further to the interior of cratons, except in cases where the cratonic lithosphere has been weakened, such as in the Rio Negro-
595   Juruena belt. The capacity of a craton to undergo reworking or deformation seems to hinge on the specific tectonic conditions they have experienced since their Precambrian consolidation.

Author contribution:

Ana Fonseca: Conceptualization, Formal analysis, Investigation, Visualization, Writing – original draft preparation

Simon Nachtergaele: Conceptualization, Formal analysis, Validation, Writing – review & editing

600 Amed Bonilla: Conceptualization, Writing – review & editing

Stijn Dewaele: Conceptualization, Writing – review & editing

Johan De Grave: Conceptualization, Supervision, Resources, Data curation, Writing – review & editing

Competing interests:

The authors declare that they have no conflict of interest.

605 **Acknowledgments**

SN was funded by a PhD scholarship from the Research Foundation Flanders (FWO Vlaanderen) number 1161721N. The research of ABP was funded by a PhD scholarship from Minciencias (before Colciencias) number 647-2014. Zeze Amaya and Jose A. Franco are thanked for assistance during sampling.

References

610 Abbey, A. L., Wildman, M., Stevens Goddard, A. L., and Murray, K. E.: Thermal history modeling techniques and interpretation strategies: Applications using QTQt, Geosphere, 19, 493–530, https://doi.org/10.1130/GES02528.1, 2023.

Almeida, M. E., and Mendes, T. M. A.: Geological and mineral resources map of South America: sheet NA.19 - Pico da Neblina (preliminary version). Geological Survey of Brazil – CPRM, 2021.

Amaya, S., Zuluaga, C. A., and Bernet, M.: New fission-track age constraints on the exhumation of the central Santander

615 Massif: Implications for the tectonic evolution of the Northern Andes, Colombia, Lithos, 282–283, 388–402, https://doi.org/10.1016/j.lithos.2017.03.019, 2017.

Artemieva, I. M. and Vinnik, L. P.: Density structure of the cratonic mantle in southern Africa: 1. Implications for dynamic topography, Gondwana Res., 39, 204–216, https://doi.org/10.1016/j.gr.2016.03.002, 2016.

Artemieva, I. M.: Global $1° \times 1°$ thermal model TC1 for the continental lithosphere: Implications for lithosphere secular

620 evolution, Tectonophysics, 416, 245–277, https://doi.org/10.1016/j.tecto.2005.11.022, 2006.

Ault, A. K., Flowers, R. M., and Bowring, S. A.: Phanerozoic surface history of the Slave craton, Tectonics, 32, 1066–1083, https://doi.org/10.1002/tect.20069, 2013.

Bande, A., Horton, B. K., Ramirez, J. C., Mora, A., Parra, M., and Stockli, D. F.: Clastic deposition, provenance, and sequence of Andean thrusting in the frontal Eastern Cordillera and Llanos foreland basin of Colombia, Geol. Soc. Am. Bull., 124,

625 59–76, https://doi.org/10.1130/B30412.1, 2012.

Basile, C., Mascle, J., and Guiraud, R.: Phanerozoic geological evolution of the Equatorial Atlantic domain. Journal of African Earth Sciences, 43(1–3), 275–282. https://doi.org/10.1016/j.jafrearsci.2005.07.011, 2005

Bedle, H., Cooper, C. M., and Frost, C. D.: Nature Versus Nurture: Preservation and Destruction of Archean Cratons, Tectonics, 40, 1–38, https://doi.org/10.1029/2021TC006714, 2021.

630 Belton, D. X. and Raab, M. J.: Cretaceous reactivation and intensified erosion in the Archean–Proterozoic Limpopo Belt, demonstrated by apatite fission track thermochronology, Tectonophysics, 480, 99–108, https://doi.org/10.1016/j.tecto.2009.09.018, 2010.

Belton, D. X.: The low temperature thermochronology of cratonic terranes, (PhD Thesis), University of Melbourne, Melbourne, Australia, 2006

635 Bleeker, W.: The late Archean record: a puzzle in ca. 35 pieces, Lithos, 71, 99–134, https://doi.org/10.1016/j.lithos.2003.07.003, 2003.

Bonilla, A., Franco, J. A., Cramer, T., Poujol, M., Cogné, N., Nachtergaele, S., and De Grave, J.: Apatite LA-ICP-MS U–Pb and fission-track geochronology of the Caño Viejita gabbro in E-Colombia: Evidence for Grenvillian intraplate rifting and Jurassic exhumation in the NW Amazonian Craton, J. South Am. Earth Sci., 98, 102438, 640 https://doi.org/10.1016/j.jsames.2019.102438, 2020.

Bonilla, A., Cramer, T., De Grave, J., Alessio, B., Glorie, S., and Kroonenberg, S.: The NW Amazonian Craton in Guainía and Vaupés departments, Colombia: Transition between orogenic to anorogenic environments during the Paleo-Mesoproterozoic, Precambrian Res., 360, 106223, https://doi.org/10.1016/j.precamres.2021.106223, 2021.

Bonilla, A., Franco Victoria, J. A., Cramer, T., De Grave, J., Nachtergaele, S., Cogné, N., and Piraquive, A.: The NW 645 Amazonian Craton in Guainía and Vaupés departments, Colombia: Evidence of a Mesoproterozoic thermal event from apatite LA-ICP-MS U-Pb geochronology and its relation to continental rifting, Precambrian Res., 395, 107148, https://doi.org/10.1016/j.precamres.2023.107148, 2023.

Buiter, S. J. H. and Torsvik, T. H.: A review of Wilson Cycle plate margins: A role for mantle plumes in continental break-up along sutures?, Gondwana Res., 26, 627–653, https://doi.org/10.1016/j.gr.2014.02.007, 2014.

650 Buiter, S. J. H., Brune, S., Keir, D., and Peron-Pinvidic, G.: Rifting Continents, in: Dynamics of Plate Tectonics and Mantle Convection, Elsevier, 459–481, https://doi.org/10.1016/B978-0-323-85733-8.00016-0, 2023.

Bustamante, C., Archanjo, C. J., Cardona, A., and Vervoort, J. D.: Late Jurassic to Early Cretaceous plutonism in the Colombian Andes: A record of long-term arc maturity, Geol. Soc. Am. Bull., 128, 1762–1779, https://doi.org/10.1130/B31307.1, 2016.

655 Cardona, A., Valencia, V., Bustamante, C., García-Casco, A., Ojeda, G., Ruiz, J., Saldarriaga, M., and Weber, M.: Tectonomagmatic setting and provenance of the Santa Marta Schists, northern Colombia: Insights on the growth and approach of Cretaceous Caribbean oceanic terranes to the South American continent, J. South Am. Earth Sci., 29, 784–804, https://doi.org/10.1016/j.jsames.2009.08.012, 2010.

Cawood, P. A. and Pisarevsky, S. A.: Was Baltica right-way-up or upside-down in the Neoproterozoic?, J. Geol. Soc. London.,
660   163, 753–759, https://doi.org/10.1144/0016-76492005-126, 2006.

CDA, departamento del Vaupés y PNUD: Plan Integral de Gestión del Cambio Climático para el departamento del Vaupés.
191 páginas. Mitú, Vaupés, 2020.

Cediel, F. and Shaw, R. P.: Geology and Tectonics of Northwestern South America, edited by: Cediel, F. and Shaw, R. P.,
Springer International Publishing, Cham, 1010 pp., https://doi.org/10.1007/978-3-319-76132-9, 2019.

665   Cediel, F., Shaw, R. P., and Cáceres, C.: Tectonic assembly of the Northern Andean Block, in: Bartolin, C., Buffler, R. T., and
Blickwede, J. (eds) The circum-Gulf of Mexico and the Caribbean: hydrocarbon habitats, basin formation, and plate
tectonics. AAPG Memoir 79:815–848, 2003.

Chimpliganond, C., Assumpção, M., Von Huelsen, M., and França, G. S.: The intracratonic Caraíbas–Itacarambi earthquake
of December 09, 2007 (4.9 mb), Minas Gerais State, Brazil, Tectonophysics, 480, 48–56,
670   https://doi.org/10.1016/j.tecto.2009.09.016, 2010.

Chorowicz, J.: The East African rift system In: Catuneanu, O., Guiraud, R., Eriksson, P., Thomas, B., Shone, R. W., Key, R.
(Eds.), Phanerozoic Evolution of Africa, J. Afr. Earth Sc. 43, 379–410, 2005.

Rønnevik, C., Ksienzyk, A. K., Fossen, H., Jacobs, J: Thermal evolution and exhumation history of the Uncompahgre Plateau
(northeastern Colorado Plateau), based on apatite fission track and (U-Th)-He thermochronology and zircon U-Pb dating.
675   Geosphere, 13 (2),518–537, doi: https://doi.org/10.1130/GES01415.1, 2017.

Coira, B., Davidson, J., Mpodozis, C., and Ramos, V.: Tectonic and magmatic evolution of the Andes of northern Argentina
and Chile, Earth-Science Rev., 18, 303–332, https://doi.org/10.1016/0012-8252(82)90042-3, 1982.

Cooper, M. A., Addison, F. T., Alvarez, R., Coral, M., Graham, R. H., Hayward, A. B., Howe, S., Martinez, J., Naar, J., Penas,
R., Pulham, A. J., and Taborda, A.: Basin Development and Tectonic History of the Llanos Basin, Eastern Cordillera, and
680   Middle Magdalena Valley, Colombia, Am. Assoc. Pet. Geol. Bull., 79, 1421–1443, https://doi.org/10.1306/7834D9F4-
1721-11D7-8645000102C1865D, 1995.

Cordani, U. G. and Teixeira, W.: Proterozoic accretionary belts in the Amazonian Craton, in: Memoir of the Geological Society
of America, vol. 200, 297–320, https://doi.org/10.1130/2007.1200(14), 2007.

Cordani, U. G., Sato, K., Sproessner, W., and Fernandes, F. S.: U-Pb zircon ages of rocks from the Amazonas Territory of
685   Colombia and their bearing on the tectonic history of the NW sector of the Amazonian Craton, 5–35 pp.,
https://doi.org/10.1590/2317-4889201620150012, 2016.

Cordani, U. G., Teixeira, W., D'Agrella-Filho, M. S., and Trindade, R. I.: The position of the Amazonian Craton in
supercontinents. Gondwana Research, 15(3–4), 396–407. https://doi.org/10.1016/j.gr.2008.12.005, 2009.

Granot, R. and Dyment, J.: The Cretaceous opening of the South Atlantic Ocean, Earth Planet. Sci. Lett., 414, 156–163,
690   https://doi.org/10.1016/j.epsl.2015.01.015, 2015.

Daly, M. C., Green, P., Watts, A. B., Davies, O., Chibesakunda, F., and Walker, R.: Tectonics and Landscape of the Central African Plateau and their Implications for a Propagating Southwestern Rift in Africa. Geochemistry, Geophysics, Geosystems, 21(6), 2020.

Davies, J. H. F. L., Marzoli, A., Bertrand, H., Youbi, N., Ernesto, M., and Schaltegger, U.: End-Triassic mass extinction started by intrusive CAMP activity. Nature Communications, 8. https://doi.org/10.1038/ncomms15596, 2017.

De Corte, F. de, Bellemans, F., Haute, P. van den, Ingelbrecht, C., and Nicholl, C.: A New U Doped Glass Certified By the European Commission for the Calibration of Fission-Track Dating, in: Advances in Fission-Track Geochronology, vol. 10, edited by: van den Haute, P. and de Corte, F., Springer, Dordrecht, 1998.

Deckart, K., Féraud, G., and Bertrand, H.: Age of Jurassic continental tholeiites of French Guyana, Surinam and Guinea: Implications for the initial opening of the Central Atlantic Ocean, Earth Planet. Sci. Lett., 150, 205–220, https://doi.org/10.1016/s0012-821x(97)00102-7, 1997.

Derycke, A., Gautheron, C., Barbarand, J., Bourbon, P., Aertgeerts, G., Simon-Labric, T., Sarda, P., Pinna-Jamme, R., Boukari, C., and Haurine, F.: French Guiana margin evolution: From Gondwana break-up to Atlantic opening, Terra Nov., 33, 415–422, https://doi.org/10.1111/ter.12526, 2021.

Ding, L., Kapp, P., Cai, F., Garzione, C. N., Xiong, Z., Wang, H., and Wang, C.: Timing and mechanisms of Tibetan Plateau uplift. Nature Reviews Earth & Environment, 3(10), 652-667, 2022.

Donelick, R. A.: Crystallographic orientation dependence of mean etchable fission track length in apatite: an empirical model and experimental observations, Am. Mineral., 76, 83–91, 1991.

Ebinger, C., and Christopher A. S.: Continental rift basins: the East African perspective, in: Busby, C., and Azor, A., Tectonics of sedimentary basins: Recent advances, 2011.

Fernie, N., Glorie, S., Jessell, M. W., and Collins, A. S.: Thermochronological insights into reactivation of a continental shear zone in response to Equatorial Atlantic rifting (northern Ghana), Sci. Rep., 8, 16619, https://doi.org/10.1038/s41598-018-34769-x, 2018.

Figueiredo, R. F. de, Santos, T. J. S. dos, and Tonetto, E. M.: Petrology, geochemistry and U-Pb zircon and baddeleyite ages of the alkaline rocks from the central-southern Guyana Shield, northern Amazonian Craton, J. South Am. Earth Sci., 86, 461–474, https://doi.org/10.1016/j.jsames.2018.08.001, 2018.

Fleischer, R. L., Price, P. B., and Walker, R. M.: Nuclear tracks in solids: Principles and applications, University of California Press, Berkeley, Calif., 626 pp., 1975.

Flowers, R. M.: The enigmatic rise of the Colorado Plateau, Geology, 38, 671–672, https://doi.org/10.1130/focus072010.1, 2010.

Foley, S. F.: Rejuvenation and erosion of the cratonic lithosphere, Nat. Geosci., 1, 503–510, https://doi.org/10.1038/ngeo261, 2008.

Fonseca, A. C., Piffer, G. V., Nachtergaele, S., Van Ranst, G., De Grave, J., and Novo, T. A.: Devonian to Permian post-orogenic denudation of the Brasília Belt of West Gondwana: insights from apatite fission track thermochronology, J. Geodyn., 137, https://doi.org/10.1016/j.jog.2020.101733, 2020.

Fonseca, A. C. L., Novo, T. A., Nachtergaele, S., Fonte-Boa, T. M. R., Van Ranst, G., and De Grave, J.: Differential Phanerozoic evolution of cratonic and non-cratonic lithosphere from a thermochronological perspective: São Francisco Craton and marginal orogens (Brazil), Gondwana Res., 93, 106–126, https://doi.org/10.1016/j.gr.2021.01.006, 2021.

Van Ranst, G., Fonseca, A. C., Tack, L., Delvaux, D., Baudet, D., Kitambala, N. Y., Pay, A. L., and De Grave, J.: Exhumation of the passive margin of the DR Congo during pre- and post- Gondwana breakup: Evidence from low-temperature thermochronology, geology and geomorphology, Geomorphology, 398, 108067, https://doi.org/10.1016/j.geomorph.2021.108067, 2022.

Gallagher, K. and Brown, R.: Denudation and uplift at passive margins: the record on the Atlantic Margin of southern Africa, 835–859, 1999.

Gallagher, K., Brown, R., and Johnson, C.: Fission track analysis and its applications to geological problems, Annu. Rev. Earth Planet. Sci., 26, 519–572, https://doi.org/10.1146/annurev.earth.26.1.519, 1998.

Gallagher, K.: Transdimensional inverse thermal history modeling for quantitative thermochronology, J. Geophys. Res., 117, 1–16, https://doi.org/10.1029/2011JB008825, 2012.

Gleadow, A. J. W. and Duddy, I. R.: Fission track analysis: a new tool for the evaluation of thermal histories and hydrocarbon potential: APEA Journal, 23, 93–102, 1981.

Gleadow, A. J. W. and Brown, R. W.: Fission track thermochronology and the long-term denudational response to tectonics, in: Geomorphology and Global Tectonics, edited by: M.J. Summerfield, Wiley, New York, 57–75, 2000.

Gleadow, A. J. W., Duddy, I. R., Green, P. F., and Lovering, J. F.: Confined fission track lengths in apatite: a diagnostic tool for thermal history analysis, Contrib. to Mineral. Petrol., 94, 405–415, https://doi.org/10.1007/BF00376334, 1986.

Gomes, C. H. and Almeida, D.: New insights into the Gondwana breakup at the Southern South America by apatite fission-track analyses, Adv. Geosci., 47, 1–15, https://doi.org/10.5194/adgeo-47-1-2019, 2019.

Gómez, J., Schobbenhaus, C., and Montes, N.E.: Geological Map of South America 2019. Scale 1:5 000 000. Commission for the Geological Map of the World (CGMW), Servicio Geológico Colombiano and Serviço Geológico do Brasil. Paris, France. https://doi.org/10.32685/10.143.2019.929, 2019

Gordon, A., Destro, N., and Heilbron, M.: The Recôncavo-Tucano-Jatobá Rift and Associated Atlantic Continental Margin Basins, in: Heilbron, M., Cordani, U., and Alkmim, F. (eds): São Francisco Craton, Eastern Brazil. Regional Geology Reviews. Springer, Cham. https://doi.org/10.1007/978-3-319-01715-0_9, 2017.

Green, P., Duddy, I., and Japsen, P.: Episodic kilometre-scale burial and exhumation and the importance of missing section. Earth-Science Reviews, 234, 104226, 2022.

Green, P. F., Duddy, I. R., Gleadow, A. J. W., Tingate, P. R. and Laslett, G. M.,: Fission-track annealing in apatite: track length measurements and the form of the Arrhenius plot, Nuclear Tracks, 10, 323–328, 1985.

760 Guerrero, J., Mejía-Molina, A., and Osorno, J.: Detrital U-Pb provenance, mineralogy, and geochemistry of the Cretaceous Colombian back-arc basin, in: J. Gómez, and A. O. Pinilla-Pachón (eds.): The geology of Colombia, Vol. 2 Mesozoic. Servicio Geológico Colombiano, Publicaciones Geológicas Especiales, 2020.

Gutiérrez, E. G., Horton, B. K., Vallejo, C., Jackson, L. J., and George, S. W. M.: Provenance and geochronological insights into Late Cretaceous-Cenozoic foreland basin development in the Subandean Zone and Oriente Basin of Ecuador, in:
765 Andean Tectonics, Elsevier, 237–268, https://doi.org/10.1016/B978-0-12-816009-1.00011-3, 2019.

Gunnell, Y.: Radiometric ages of laterites and constraints on long-term denudation rates in West Africa, Geology, 31, 131, https://doi.org/10.1130/0091-7613(2003)031<0131:RAOLAC>2.0.CO;2, 2003.

Harman, R., Gallagher, K., Brown, R., Raza, A., and Bizzi, L.: Accelerated denudation and tectonic/geomorphic reactivation of the cratons of northeastern Brazil during the Late Cretaceous, J. Geophys. Res. Solid Earth, 103, 27091–27105,
770 https://doi.org/10.1029/98JB02524, 1998.

Horton, B. K., Saylor, J. E., Nie, J., Mora, A., Parra, M., Reyes-Harker, A., and Stockli, D. F.: Linking sedimentation in the northern Andes to basement configuration, Mesozoic extension, and Cenozoic shortening: Evidence from detrital zircon U-Pb ages, Eastern Cordillera, Colombia, Bull. Geol. Soc. Am., 122, 1423–1442, https://doi.org/10.1130/B30118.1, 2010.

Horton, B. K.: Sedimentary record of Andean mountain building, Earth-Science Rev., 178, 279–309,
775 https://doi.org/10.1016/j.earscirev.2017.11.025, 2018.

Hu, J., Liu, L., Faccenda, M., Zhou, Q., Fischer, K. M., Marshak, S., and Lundstrom, C.: Modification of the Western Gondwana craton by plume-lithosphere interaction, Nat. Geosci., 11, 203–210, https://doi.org/10.1038/s41561-018-0064-1, 2018.

Hurford, A. J. and Hammerschmidt, K.: Ar40/Ar39 and K/Ar dating of the bishop and fish canyon tuffs: Calibration ages for
780 fission-track dating standards, Chem. Geol. Isot. Geosci. Sect., 58, 23–32, https://doi.org/10.1016/0168-9622(85)90024-7, 1985.

Hurtado, C., Roddaz, M., Santos, R. V., Baby, P., Antoine, P. O., and Dantas, E. L.: Cretaceous-early Paleocene drainage shift of Amazonian rivers driven by Equatorial Atlantic Ocean opening and Andean uplift as deduced from the provenance of northern Peruvian sedimentary rocks (Huallaga basin), Gondwana Res., 63, 152–168,
785 https://doi.org/10.1016/j.gr.2018.05.012, 2018.

Ibanez-Mejia, M., Ruiz, J., Valencia, V. A., Cardona, A., Gehrels, G. E., and Mora, A. R.: The Putumayo Orogen of Amazonia and its implications for Rodinia reconstructions: New U-Pb geochronological insights into the Proterozoic tectonic evolution of northwestern South America, Precambrian Res., 191, 58–77, https://doi.org/10.1016/j.precamres.2011.09.005, 2011.

790 Jaimes, E. and de Freitas, M.: An Albian-Cenomanian unconformity in the northern Andes: Evidence and tectonic significance, J. South Am. Earth Sci., 21, 466–492, https://doi.org/10.1016/j.jsames.2006.07.011, 2006.

Japsen, P., Bonow, J. M., Green, P. F., Cobbold, P. R., Chiossi, D., Lilletveit, R., Magnavita, L. P. and Pedreira, A. J.: Episodic burial and exhumation history of NE Brazil after opening of the South Atlantic. GSA Bulletin, 124: 800-816, 2012. ~~Japsen, P., Chalmers, J. A., Green, P. F., and Bonow, J. M.: Elevated, passive continental margins: Not rift shoulders, but expressions of episodic, post-rift burial and exhumation, Glob. Planet. Change, 90-91, 73-86, https://doi.org/10.1016/j.gloplacha.2011.05.004, 2012.~~

Jelinek, A. R., Chemale, F., van der Beek, P. A., Guadagnin, F., Cupertino, J. A., and Viana, A.: Denudation history and landscape evolution of the northern East-Brazilian continental margin from apatite fission-track thermochronology, J. South Am. Earth Sci., 54, 158–181, https://doi.org/10.1016/j.jsames.2014.06.001, 2014.

Jelinek, A. R., Corrêa-Gomes, L. C., and Bicca, M. M.: Evolução termotectônica fanerozoica da margem continental na área do Rifte Recôncavo-Tucano-Jatobá, Pesqui. em Geociências, 47, https://doi.org/10.22456/1807-9806.101330, 2020.Jiménez et al., 2020

Johansson, Å.: From Rodinia to Gondwana with the "SAMBA" model-A distant view from Baltica towards Amazonia and beyond, Precambrian Res., 244, 226–235, https://doi.org/10.1016/j.precamres.2013.10.012, 2014.

Odoh, S., Saylor, J. E., Higuera, C., Copeland, P., and Lapen, T. J.: Discriminating mechanisms for coarse clastic progradation in the Colombian foreland basin using detrital zircon double dating, Elsevier Inc., 133–171 pp., https://doi.org/10.1016/B978-0-12-816009-1.00008-3, 2019.

Kasanzu, C. H.: Apatite fission track and (U-Th)/He thermochronology from the Archean Tanzania Craton: Contributions to cooling histories of Tanzanian basement rocks, Geosci. Front., 8, 999–1007, https://doi.org/10.1016/j.gsf.2016.09.007, 2017.

Ketcham, R. A., Carter, A., Donelick, R. A., Barbarand, J., and Hurford, A. J.: Improved modeling of fission-track annealing in apatite, Am. Mineral., 92, 799–810, https://doi.org/10.2138/am.2007.2281, 2007a.

Ketcham, R. A., Carter, A., Donelick, R. A., Barbarand, J., and Hurford, A. J.: Improved measurement of fission-track annealing in apatite using c-axis projection, Am. Mineral., 92, 789–798, https://doi.org/10.2138/am.2007.2280, 2007b.

Ketcham, R. A.: Forward and inverse modeling of low-temperature thermochronometry data, Rev. Mineral. Geochemistry, 58, 275–314, https://doi.org/10.2138/rmg.2005.58.11, 2005.

Kohn, B. and Gleadow, A.: Application of Low-Temperature Thermochronology to Craton Evolution, in: Fission-Track Thermochronology and its Application to Geology, edited by: Malusà, M. G. and Fitzgerald, P. G., Springer Textbooks in Earth Sciences, Geography and Environment, 373–393, https://doi.org/10.1007/978-3-319-89421-8_21, 2019.

Kollenz, S., Glasmacher, U. A., Rossello, E. A., Stockli, D. F., Schad, S., and Pereyra, R. E.: Thermochronological constraints on the Cambrian to recent geological evolution of the Argentina passive continental margin, Tectonophysics, 716, 182–203, https://doi.org/10.1016/j.tecto.2016.11.019, 2017.

Kroonenberg, S. B.: A Grenvillian granulite belt in the Colombian Andes and its relation to the Guiana Shield: Geologie en Mijnbouw, v. 61, p. 325–333, 1982.

Kusky, T. M., Windley, B. F., Wang, L., Wang, Z., Li, X., and Zhu, P.: Flat slab subduction, trench suction, and craton destruction: Comparison of the North China, Wyoming, and Brazilian cratons, Tectonophysics, 630, 208–221, https://doi.org/10.1016/j.tecto.2014.05.028, 2014.

Kusznir, N. J. and Park, R. G.: Intraplate lithosphere deformation and the strength of the lithosphere, Geophys. J. Int., 79, 513–
830   538, https://doi.org/10.1111/j.1365-246X.1984.tb02238.x, 1984.

Laslett G., Green P., Duddy I. and Gleadow A.: Thermal annealing of fission tracks in apatite. Chem. Geol. 65, 1–13, 1987.

León, S., Cardona, A., Mejía, D., Botello, G. E., Villa, V., Collo, G., Valencia, V., Zapata, S., and Avellaneda-Jiménez, D. S.: Source area evolution and thermal record of an Early Cretaceous back-arc basin along the northwesternmost Colombian Andes, J. South Am. Earth Sci., 94, 102229, https://doi.org/10.1016/j.jsames.2019.102229, 2019.

835   Leprêtre, R., Barbarand, J., Missenard, Y., Leparmentier, F., and Frizon De Lamotte, D.: Vertical movements along the northern border of the West African Craton: The Reguibat Shield and adjacent basins, Geol. Mag., 151, 885–898, https://doi.org/10.1017/S0016756813000939, 2014.

Leprêtre, R., Missenard, Y., Barbarand, J., Gautheron, C., Saddiqi, O., and Pinna-Jamme, R.: Postrift history of the eastern central Atlantic passive margin: Insights from the Saharan region of South Morocco, J. Geophys. Res. Solid Earth, 120,
840   4645–4666, https://doi.org/10.1002/2014JB011549, 2015.

Li, Z. X., Bogdanova, S. V., Collins, A. S., Davidson, A., De Waele, B., Ernst, R. E., Fitzsimons, I. C. W., Fuck, R. A., Gladkochub, D. P., Jacobs, J., Karlstrom, K. E., Lu, S., Natapov, L. M., Pease, V., Pisarevsky, S. A., Thrane, K., and Vernikovsky, V.: Assembly, configuration, and break-up history of Rodinia: A synthesis, Precambrian Res., 160, 179–210, https://doi.org/10.1016/j.precamres.2007.04.021, 2008.

845   Liu, L., Morgan, J. P., Xu, Y., and Menzies, M.: Craton Destruction 1: Cratonic Keel Delamination Along a Weak Midlithospheric Discontinuity Layer, J. Geophys. Res. Solid Earth, 123, 10,040-10,068, https://doi.org/10.1029/2017JB015372, 2018.

Macgregor, D.: History of the development of the East African Rift System: A series of interpreted maps through time, J. African Earth Sci., 101, 232–252, https://doi.org/10.1016/j.jafrearsci.2014.09.016, 2015.

850   Machado, J. P. S. L., Jelinek, A. R., Stephenson, R., Gaucher, C., Bicca, M. M., Chiglino, L., and Genezini, F. A.: Low-temperature thermochronology of the South Atlantic margin along Uruguay and its relation to tectonic events in West Gondwana, Tectonophysics, 105, 228439, https://doi.org/10.1016/j.tecto.2020.228439, 2020.

Mackintosh, V., Kohn, B., Gleadow, A., and Gallagher, K.: Long-term reactivation and morphotectonic history of the Zambezi Belt, northern Zimbabwe, revealed by multi-method thermochronometry, Tectonophysics, 750, 117–136,
855   https://doi.org/10.1016/j.tecto.2018.11.009, 2019.

Maloney, K. T., Clarke, G. L., Klepeis, K. A., and Quevedo, L.: The Late Jurassic to present evolution of the Andean margin: Drivers and the geological record, Tectonics, 32, 1049–1065, https://doi.org/10.1002/tect.20067, 2013.

Manatschal, G., Lavier, L., and Chenin, P.: The role of inheritance in structuring hyperextended rift systems: Some considerations based on observations and numerical modeling, Gondwana Res., 27, 140–164, https://doi.org/10.1016/j.gr.2014.08.006, 2015.

Martin-Gombojav, N. and Winkler, W.: Recycling of proterozoic crust in the andean amazon foreland of Ecuador: Implications for orogenic development of the Northern Andes, Terra Nov., 20, 22–31, https://doi.org/10.1111/j.1365-3121.2007.00782.x, 2008.

Marzoli, A., Renne, P. R., Piccirillo, E. M., Ernesto, M., Bellieni, G., and De Min, A.: Extensive 200-million-year-old continental flood basalts of the Central Atlantic Magmatic Province, Science (80-.)., 284, 616–618, https://doi.org/10.1126/science.284.5414.616, 1999.

Marzoli, A., Callegaro, S., Dal Corso, J., Davies, J. H. F. L., Chiaradia, M., Youbi, N., Bertrand, H., Reisberg, L., Merle, R., and Jourdan, F.: The Central Atlantic Magmatic Province (CAMP): A review, in: L. H. Tanner (Ed.), The Late Triassic World (pp. 91– 125). Springer International Publishing, 2018.

McDowell, F. W., McIntosh, W. C., and Farley, K. A.: A precise 40Ar–39Ar reference age for the Durango apatite (U–Th)/He and fission-track dating standard, Chem. Geol., 214, 249–263, https://doi.org/10.1016/j.chemgeo.2004.10.002, 2005.

Mendes, T., Nascimento, R., Veras, R., Almeida, M., and Knauer, L.: Geological knowledge advances on the Alto Rio Negro region, northwestern Amazonian Craton, Brazil: a review, J. Geol. Surv. Brazil, 4, 209–222, https://doi.org/10.29396/jgsb.2021.v4.n3.2, 2021.

Mora, A., Parra, M., Strecker, M. R., Kammer, A., Dimaté, C., and Rodríguez, F.: Cenozoic contractional reactivation of Mesozoic extensional structures in the Eastern Cordillera of Colombia, Tectonics, 25, 1–19, https://doi.org/10.1029/2005TC001854, 2006.

Moreno-López, M. C. and Escalona, A.: Precambrian-Pleistocene tectono-stratigraphic evolution of the southern Llanos Basin, Colombia, Am. Assoc. Pet. Geol. Bull., 99, 1473–1501, https://doi.org/10.1306/11111413138, 2015.

Noble, W. P., Foster, D. A., and Gleadow, A. J. W.: The post-Pan-African thermal and extensional history of crystalline basement rocks in eastern Tanzania, Tectonophysics, 275, 331–350, https://doi.org/10.1016/S0040-1951(97)00026-7, 1997.

Noble, W. P.: Post Pan African tectonic evolution of eastern Africa: An apatite fission track study, (PhD thesis). Melbourne, Australia, La Trobe University, 1997.

Oukassou, M., Saddiqi, O., Barbarand, J., Sebti, S., Baidder, L., and Michard, A.: Post-Variscan exhumation of the Central Anti-Atlas (Morocco) constrained by zircon and apatite fission-track thermochronology, Terra Nov., 25, 151–159, https://doi.org/10.1111/ter.12019, 2013.

Pachón-Parra, L. F., Mann, P., and Cardozo, N.: Regional subsurface mapping and 3D flexural modeling of the obliquely-converging Putumayo Foreland Basin, Southern Colombia, Interpretation, 8, 1–115, https://doi.org/10.1190/int-2020-0021.1, 2020.

Pankhurst, R. J., Riley, T. R., Fanning, C. M., and Kelly, S. P.: Episodic Silicic Volcanism in Patagonia and the Antarctic Peninsula: Chronology of Magmatism Associated with the Break-up of Gondwana, J. Petrol., 41, 605–625, https://doi.org/10.1093/petrology/41.5.605, 2000.

Horton, B. K.: Sedimentary record of Andean mountain building, Earth-Science Rev., 178, 279–309, https://doi.org/10.1016/j.earscirev.2017.11.025, 2018.

Parsons, T.: Chapter 7 The basin and range province, in: Developments in Geotectonics, vol. 25, 277–XV, https://doi.org/10.1016/S0419-0254(06)80015-7, 2006.

Pérez-Consuegra, N., Hoke, G. D., Mora, A., Fitzgerald, P., Sobel, E. R., Sandoval, J. R., Glodny, J., Valencia, V., Parra, M., and Zapata, S.: The Case for Tectonic Control on Erosional Exhumation on the Tropical Northern Andes Based on Thermochronology Data, Tectonics, 40, 1–24, https://doi.org/10.1029/2020TC006652, 2021.

Pérez-Gussinyé, M., Swain, C. J., Kirby, J. F., and Lowry, A. R.: Spatial variations of the effective elastic thickness, T e , using multitaper spectral estimation and wavelet methods: Examples from synthetic data and application to South America, Geochemistry, Geophys. Geosystems, 10, n/a-n/a, https://doi.org/10.1029/2008GC002229, 2009.

Quigley, M. C., Karlstrom, K. E., Kelley, S., and Heizler, M.: Timing and mechanisms of basement uplift and exhumation in the Colorado Plateau-Basin and Range transition zone, Virgin Mountain anticline, Nevada-Arizona, Spec. Pap. Geol. Soc. Am., 463, 311–329, https://doi.org/10.1130/2010.2463(14), 2010.

Ramos, V.A., and Aleman, A.: Tectonic evolution of the Andes, in: Cordani, U.G. (ed.): Tectonc Evolution of South America, Rio de Janeiro, p. 856, 2000.

Reis, N. J., Almeida, M. E., Riker, S. L., and Ferreira, A.L.,: Geologia e recursos minerais do estado do Amazonas, 2006.

Rooney, T. O.: The Cenozoic magmatism of East Africa: Part III – Rifting of the craton, Lithos, 360–361, 105390, https://doi.org/10.1016/j.lithos.2020.105390, 2020.

Sahu, H. S., Raab, M. J., Kohn, B. P., Gleadow, A. J. W., and Kumar, D.: Denudation history of Eastern Indian peninsula from apatite fission track analysis: Linking possible plume-related uplift and the sedimentary record, Tectonophysics, 608, 1413–1428, https://doi.org/10.1016/j.tecto.2013.06.002, 2013.

Salazar-Mora, C. A., Huismans, R. S., Fossen, H., and Egydio-Silva, M.: The Wilson Cycle and Effects of Tectonic Structural Inheritance on Rifted Passive Margin Formation, Tectonics, 37, 3085–3101, https://doi.org/10.1029/2018TC004962, 2018.

Santos, J. O. S., Hartmann, L. A., Gaudette, H. E., Groves, D. I., Mcnaughton, N. J., and Fletcher, I. R.: A New Understanding of the Provinces of the Amazon Craton Based on Integration of Field Mapping and U-Pb and Sm-Nd Geochronology, Gondwana Res., 3, 453–488, https://doi.org/10.1016/S1342-937X(05)70755-3, 2000.

Santos, J. O. S., Hartmann, L. A., Faria, M. S. G., Riker, S. R., Souza, M. M., Almeida, M. E., and McNaughton, N. J.: A compartimentação do Craton Amazonas em províncias: avanços ocorridos no período 2000-2006. In: SBG-NO, Simpósio de Geologia da Amazônia, 9, Belém, CD-Rom, 2006.

Sapin, F., Davaux, M., Dall'asta, M., Lahmi, M., Baudot, G., and Ringenbach, J. C.: Post-rift subsidence of the French Guiana hyper-oblique margin: From rift-inherited subsidence to Amazon deposition effect, Geol. Soc. Spec. Publ., 431, 125–144,

925   https://doi.org/10.1144/SP431.11, 2016.

Sarmiento-Rojas, L. F., Van Wess, J. D., and Cloetingh, S.: Mesozoic transtensional basin history of the Eastern Cordillera, Colombian Andes: Inferences from tectonic models, J. South Am. Earth Sci., 21, 383–411, https://doi.org/10.1016/j.jsames.2006.07.003, 2006.

Sloss, L. L.: Tectonic episodes of cratons: conflicting North American concepts. Terra Nova, 4(3), 320–328.

930   https://doi.org/10.1111/j.1365-3121.1992.tb00821.x, 1992.

Sloss, L. L.: Sequences in the Cratonic Interior of North America. Geological Society of America Bulletin, 74, 93–114, 1963.

Snyder, D. B., Humphreys, E., and Pearson, D. G.: Construction and destruction of some North American cratons, Tectonophysics, 694, 464–485, https://doi.org/10.1016/j.tecto.2016.11.032, 2017.

Spikings, R. A., Seward, D., Winkler, W., and Ruiz, G. M.: Low-temperature thermochronology of the northern Cordillera

935   Real, Ecuador: Tectonic insights from zircon and apatite fission track analysis, Tectonics, 19, 649–668, https://doi.org/10.1029/2000TC900010, 2000.

Spikings, R., Cochrane, R., Villagomez, D., Van der Lelij, R., Vallejo, C., Winkler, W., and Beate, B.: The geological history of northwestern South America: from Pangaea to the early collision of the Caribbean Large Igneous Province (290–75Ma), Gondwana Res., 27, 95–139, https://doi.org/10.1016/j.gr.2014.06.004, 2015.

940   Spikings, R. A., Cochrane, R., Vallejo, C., Villagomez, D., Van der Lelij, R., Paul, A., and Winkler, W.: Latest Triassic to Early Cretaceous tectonics of the Northern Andes: Geochronology, geochemistry, isotopic tracing, and thermochronology, Elsevier Inc., 173–208 pp., https://doi.org/10.1016/B978-0-12-816009-1.00009-5, 2019.

Stanley, J. R., Flowers, R. M., and Bell, D. R.: Kimberlite (U-Th)/He dating links surface erosion with lithospheric heating, thinning, and metasomatism in the southern African Plateau, Geology, 41, 1243–1246, https://doi.org/10.1130/G34797.1,

945   2013.

Stanley, J. R., Flowers, R. M., and Bell, D. R.: Erosion patterns and mantle sources of topographic change across the southern African Plateau derived from the shallow and deep records of kimberlites, Geochemistry Geophys. Geosystems, 18, 1541–1576, https://doi.org/10.1002/2014GC005684.Key, 2015.

Tassinari, C. C. G. and Macambira, M. J. B.: Geochronological provinces of the Amazonian Craton, Episodes, 22, 174–182,

950   https://doi.org/10.18814/epiiugs/1999/v22i3/004, 1999.

Teixeira, W., Tassinari, C. C. G., Cordani, U. G., and Kawashita, K.: A review of the geochronology of the Amazonian Craton: Tectonic implications, Precambrian Res., 42, 213–227, https://doi.org/10.1016/0301-9268(89)90012-0, 1989.

Tong, K., Li, Z., Zhu, L., Xu, G., Zhang, Y., Kamp, P. J., Tao, G., Yang, W., Li, J., Wang, Z., and Zhang, H.: Thermochronology constraints on the Cretaceous-Cenozoic thermo-tectonic evolution in the Gaize region, central-western

955   Tibetan Plateau: Implications for the westward extension of the proto-Tibetan Plateau. Journal of Asian Earth Sciences, 240, 105419, 2022.

Toussaint, J. F. and Restrepo, J. J.: Tectonostratigraphic Terranes in Colombia: An Update Second Part: Oceanic Terranes, Geol. Colomb., 2, 24, 2020.

Turner, J. P., Green, P. F., Holford, S. P., and Lawrence, S. R.: Thermal history of the Rio Muni (West Africa)-NE Brazil margins during continental breakup, Earth Planet. Sci. Lett., 270, 354–367, https://doi.org/10.1016/j.epsl.2008.04.002, 2008.

Vallejo, C., Tapia, D., Gaibor, J., Steel, R., Cardenas, M., Winkler, W., Valdez, A., Esteban, J., Figuera, M., Leal, J., and Cuenca, D.: Geology of the Campanian M1 sandstone oil reservoir of eastern Ecuador: A delta system sourced from the Amazon Craton, Mar. Pet. Geol., 86, 1207–1223, https://doi.org/10.1016/j.marpetgeo.2017.07.022, 2017.

Vallejo, C., Romero, C., Horton, B. K., Spikings, R. A., Gaibor, J., Winkler, W., Esteban, J. J., Thomsen, T. B., and Mariño, E.: Jurassic to Early Paleogene sedimentation in the Amazon region of Ecuador: Implications for the paleogeographic evolution of northwestern South America, Glob. Planet. Change, 204, https://doi.org/10.1016/j.gloplacha.2021.103555, 2021.

Van Der Beek, P., Mbede, E., Andriessen, P., and Delvaux, D.: Denudation history of the Malawi and Rukwa Rift flanks (East African Rift system) from apatite fission track thermochronology, J. African Earth Sci., 26, 363–385, https://doi.org/10.1016/S0899-5362(98)00021-9, 1998.

Van Ranst, G., Baert, P., Fernandes, A. C., and De Grave, J.: Technical note: Nikon–TRACKFlow, a new versatile microscope system for fission track analysis, Geochronology, 2, 93–99, https://doi.org/10.5194/gchron-2-93-2020, 2020.

Vaz, P. T., Wanderley Filho, J. R., and Bueno, G. V.: Bacia do Tacutu. Bol. Geoci.PETROBRÁS, Rio de Janeiro, 2007.

Villagómez, D. and Spikings, R.: Thermochronology and tectonics of the Central and Western Cordilleras of Colombia: Early Cretaceous-Tertiary evolution of the Northern Andes, Lithos, 160–161, 228–249, https://doi.org/10.1016/j.lithos.2012.12.008, 2013.

Villagómez, D., Spikings, R., Magna, T., Kammer, A., Winkler, W., and Beltrán, A.: Geochronology, geochemistry and tectonic evolution of the Western and Central cordilleras of Colombia, Lithos, 125, 875–896, https://doi.org/10.1016/j.lithos.2011.05.003, 2011.

Villamil, T., and Arango, C.: Integrated stratigraphy of latest Cenomanian and Early Turonian facies of Colombia, in: Pindell, J. L., and Drake, C. L. (eds): Paleogeographic evolution and non–glacial eustacy, northern South America. Society for Sedimentary Geology, Special Publication 58, p. 129–159. https:// doi.org/10.2110/pec.98.58.0129, 1998

Wagner, G. A. and Van den haute, P.: Fission Track Dating, Kluwer Academic Publishers, Dordrecht, 285 pp. pp., 1992.

Wildman, M., Brown, R., Persano, C., Beucher, R., Stuart, F. M., Mackintosh, V., Gallagher, K., Schwanethal, J., and Carter, A.: Contrasting Mesozoic evolution across the boundary between on and off craton regions of the South African plateau inferred from apatite fission track and (U-Th-Sm)/He thermochronology, J. Geophys. Res. Solid Earth, 122, 1517–1547, https://doi.org/10.1002/2016JB013478, 2017.

Wildman, M., Webster, D., Brown, R., Chardon, D., Rouby, D., Ye, J., Huyghe, D., and Dall'Asta, M.: Long-term evolution
990   of the West African transform margin: estimates of denudation from Benin using apatite thermochronology, J. Geol. Soc.
London., 176, 97–114, https://doi.org/10.1144/jgs2018-078, 2019.

Wildman, M., Brown, R., Ye, J., Chardon, D., Rouby, D., Kouamelan, A. N., and Dall'Asta, M.: Contrasting Thermal
Evolution of the West African Equatorial and Central Atlantic Continental Margins, Gondwana Res., 111, 249–264,
https://doi.org/10.1016/j.gr.2022.08.010, 2022.

995   Yang, Y., Nie, J., Miao, Y., Wan, S., and Jonell, T. N.: Tibetan Plateau uplift and environmental impacts: New progress and
perspectives. Frontiers in Earth Science, 10, 1020354, 2022.

Ye, J., Chardon, D., Rouby, D., Guillocheau, F., Dall'asta, M., Ferry, J. N., and Broucke, O.: Paleogeographic and structural
evolution of northwestern Africa and its Atlantic margins since the early Mesozoic, Geosphere, 13, 1254–1284,
https://doi.org/10.1130/GES01426.1, 2017.

1000   Zapata, S., Cardona, A., Jaramillo, J. S., Patiño, A., Valencia, V., León, S., Mejía, D., Pardo-Trujillo, A., and Castañeda, J. P.:
Cretaceous extensional and compressional tectonics in the Northwestern Andes, prior to the collision with the Caribbean
oceanic plateau, Gondwana Res., 66, 207–226, https://doi.org/10.1016/j.gr.2018.10.008, 2019.